Characterization of a fourth *Schistosoma mansoni* glutamate-gated chloride channel subunit

Hilary Byrne

Institute of Parasitology, McGill University
Ste-Anne-de-Bellevue, Quebec, Canada

November 2016

A thesis submitted to McGill University in partial fulfillment of the requirement of the degree of Masters of Science

ABSTRACT

Schistosomiasis, a neglected tropical disease caused by parasitic trematodes of the genus *Schistosoma*, affects hundreds of millions of people in developing areas of the world. Chronic schistosome infections impede growth and development, particularly in young children. The threat of resistance development to the only drug currently used to treat schistosomiasis, praziquantel (PZQ), has intensified the need for development of new schistosomicidal compounds.

Targeting the nervous system of schistosomes for drug development is promising, as it coordinates many vital parasite functions. Glutamate-gated chloride channels of *Schistosoma mansoni* (SmGluCls) have been characterized recently and are of particular interest as they have been successfully targeted in other parasites. Four *S. mansoni* SmGluCl subunits were cloned and three of these were electrophysiologically characterized in *Xenopus laevis* oocytes and immunolocalized in parasites. The research in this thesis focuses on characterizing the fourth subunit, SmGluCl-4. Research also includes development of a mammalian cell-based fluorescence assay to enable screening of chemical libraries for channel agonists and antagonists.

Two-electrode voltage clamp experiments showed that SmGluCl-4 does not form a functional homomeric receptor in oocytes; however, the subunit was localized to the surface of injected oocytes, indicating that unresponsiveness to glutamate was not due to lack of protein expression. Further experiments showed that SmGluCl-4 does not form a heteromeric receptor with other subunits. Although SmGluCl-4 does not form a functional receptor, confocal immunolocalization studies have shown that the subunit is found in both the central and peripheral nervous systems, with distribution patterns similar to the other SmGluCls, indicating

that SmGluCl-4 may have a functional role within the parasite that can not be elucidated with our current methods.

A yellow-fluorescence protein (YFP) assay to detect SmGluCl channel activity was developed by co-transfecting mammalian cells with plasmids encoding YFP and SmGluCl-2 (a subunit previously shown to form a functional glutamate receptor). Application of glutamate lead to a decrease of fluorescence, indicating functional channel activity. Future work would involve scaling this assay for use in high-throughput screening.

ABRÉGÉ

La schistosomiase est une maladie tropicale négligée causée par des parasites du genre *Schistosoma* qui affecte des centaines de millions de personnes dans les pays en voie de développement. La schistosomiase chronique entrave la croissance et le développement, particulièrement chez les enfants en bas âge. La menace de développement de résistance au seul médicament disponible pour le traitement de la schistosomiase, le PZQ, rend indispensable le développement de nouveaux agents schistosomicides.

Le système nerveux des schistosomes, étant responsable de beaucoup the fonctions vitales du parasite, est une excellente cible pour le développement de nouveaux médicaments. Les récepteurs sensitifs au L-glutamate de *Schistosoma mansoni* (SmGluCls) ont récemment été caractérisés et s'avèrent-être intéressants car ils ont été ciblés avec succès chez d'autres parasites. Quatre sous-unités SmGluCl ont été clonées et trois d'entre elles ont été caractérisées par l'électrophysiologie en utilisant des ovocytes de *Xenopus laevis* et par immulocalisation dans les parasites. La recherche effectué dans cette thèse avait pout but la caractérisation du quatrième sous-unité, SmGluCl-4. Cette recherche inclut également le développement d'un test *in vitro* avec des cellules mammifères basé sure la fluorescence afin d'identificatier des agonistes et des antagonistes des SmGluCls.

Nos expériences d'électrophysiologie ont démontré que SmGluCl-4 ne forme pas de récepteur homomérique fonctionnel dans les ovocytes. Cependant, la sous-unité a été localisée à la surface des ovocytes, indiquant que l'absence de réponse au glutamate n'était pas due à l'absence des protéines. D'autres expériences ont démontré que SmGluCl-4 ne forme pas de récepteur hétéromère avec d'autres sous-unités. Même si SmGluCl-4 ne forme pas de récepteur,

des études d'immunocalisation confocale ont démontré que la sous-unité se trouve dans les systèmes nerveux central et périphérique. De plus, la localisation de SmGluCl-4 est, semblables aux autres SmGluCls, indiquant que SmGluCl-4 pourrait exercer un rôle fonctionnel chez le parasite qui n'a pas pu être élucidé avec les méthodes utilisées dans cette thèse.

Un essai avec une protéine fluorescente jaune (YFP) a été développé pour détecter l'activité des SmGluCls. Des cellules mammifères ont été co-transfectées avec des plasmides codant YFP et SmGluCl-2 (une sous-unité qui forme un récepteur de L-glutamate). La fluorescence a diminué lors de l'application du L-glutamate, indiquant la fonctionnalité des récepteurs. Les travaux futurs comprendront la mise à l'échelle de cet essai pour son utilisation au criblage à haut débit.

ACKNOWLEDGEMENTS

I would first like to thank my supervisor, Dr. Timothy Geary, for providing me with continual guidance and encouragement, teaching me to believe in myself and my research. I have learned so much over my last few years in your lab, and I know I will take the skills I have learned from you wherever I go. For that, I am eternally grateful.

I would like to extend sincere thanks to Dr. Vanessa Dufour, without whom I would not have had a project to work on. You were always an email away, willing to help me out with anything. Your work on this project was amazing, and it inspired me to work hard to maintain the standards you set forth.

I would like to thank my advisory committee members, Dr. Paula Ribeiro and Dr. Robin Beech, for providing me with direction and for always being willing to discuss any matter relating to my work – you always had me thinking and helped me better understand the project.

I owe so much to the former and current members of the Geary/Beech lab: to Martine Ruiz Montiel, for teaching me everything you know about cell culture and helping me settle into the lab; to Thomas Duguet and Mark Kaji, for teaching me electrophysiology and always being ready to lend a hand whenever I needed help; to Dr. Maeghan O'Neill, for introducing me to Tim and letting me follow you here from UNB; and to the rest of the lab, Damian Clarke, Aynsley Merk, Clemence Ackermann, Dr. Elizabeth Ruiz Lancheros, and Dr. Cristina Ballesteros, for cheering me on or commiserating with me, whichever was the most fitting at the time.

The staff at the Institute is second to none, and without so many of you, I never would have been able to complete my project. To Serghei Dernovici, thank you for training me on the

microscopes and always being there whenever I needed help. To Kathy Keller, thank you for saving my day countless times with supplies and equipment. To Anastasia Glebov, thank you for training me to work with the mice and do infections, and for all of your help with cell culture. To Shirley Mongeau and Christiane Trudeau, you keep this place running smoothly and without you, we would all be lost.

I would like to thank Stevo Radinovic and Qi Yang from the McGill High Throughput Screening Facility for their guidance in the development of the cell assay and for providing BHK cells.

I would also like to thank the friends I have made at the Institute for making my years there some of the best of my life, especially Georgia Limniatis, Maude Dagenais, who both helped with the translation of the abstract, and Asimah Hussain, and Laura Di Gravio.

I would like to acknowledge all of the funding sources which facilitated my research: The Natural Sciences and Engineering Research Council for awarding me the Alexander Graham Bell Scholarship and for grants provided to Dr. Tim Geary, the Institute of Parasitology and the Faculty of Agricultural and Environmental Sciences for awarding me the Graduate Excellence Fellowship, the Government of Canada Research Chairs, and the Fonds de Recherche du Québec – Nature et Technologies, who supports the Centre for Host-Parasite Interactions.

Last but not least, I would like to thank some of the most important people in my life: my family and my partner. Knowing I can always count on you means the world to me.

TABLE OF CONTENTS

LIST OF ABBRIEVIATIONS

AbD	antibody diluent
ACh	acetylcholine
bp	base pairs
BSA	bovine serum albumin
Ca^{2+}	calcium
$CaCl_2$	calcium chloride
CG	cerebral ganglia
Cl^-	chloride
CNS	central nervous system
CO_2	carbon dioxide
cRNA	capped ribonucleic acid
dH_2O	distilled water
DMEM	Dulbecco's modified Eagle's medium
DNA	deoxyribonucleic acid
EC_{50}	half-maximal response
ECD	extracellular domain
ED_{50}	median effective dose
FBS	fetal bovine serum
GABA	γ-aminobutyric acid
GluCl	glutamate-gated chloride channel
HEK	human embryonic kidney
HTS	high-throughput screening
ICD	intracellular domain
IgG	immunoglobulin G
IVM	ivermection
KCl	potassium chloride
L-glu	L-glutamate
LiCl	lithium chloride
LNC	laternal nerve cord
NaCl	sodium chloride
NaI	sodium iodide
MC	main nerve cord
MDA	mass drug administration
$MgCl_2$	magnesium chloride
NN	nerve net
NTD	neglected tropical disease
OS	oral sucker
PBS	phosphate buffered saline
PFA	paraformaldehyde
pLGIC	pentameric ligand-gated ion channel
PNS	peripheral nervous system
PZQ	praziquantel
RACE	rapid amplification of cDNA ends

RNAi	RNA interference
RT	room temperature
RT-PCR	reverse transcription polymerase chain reaction
SDS	sodium dodecyl sulfate
SmGluCl	*Schistosoma mansoni* glutamate-gated chloride channel
SP	signal peptide
TC	transverse commissure
TEVC	two-electrode voltage clamp
TMD	transmembrane domain
VNC	ventral nerve cord
VS	ventral sucker
YFP	yellow fluorescent protein

LIST OF FIGURES

CHAPTER I

INTRODUCTION

INTRODUCTION

1.1. Schistosome classification and biology

Blood flukes of the genus *Schistosoma* are parasitic trematodes belonging to the phylum Platyhelminthes (Gryseels, 2012). Five species infect humans (Figure 1). The three main contributors to the schistosomiasis burden are *Schistosoma mansoni*, found throughout Africa, the Arabian Peninsula, and South America; *Schistosoma japonicum*, found in Asia; and *Schistosoma haematobium,* found in Africa and the Arabian Peninsula (Caffrey, 2007). The first two are responsible for the intestinal form of the disease, whereas the latter causes urinary schistosomiasis.

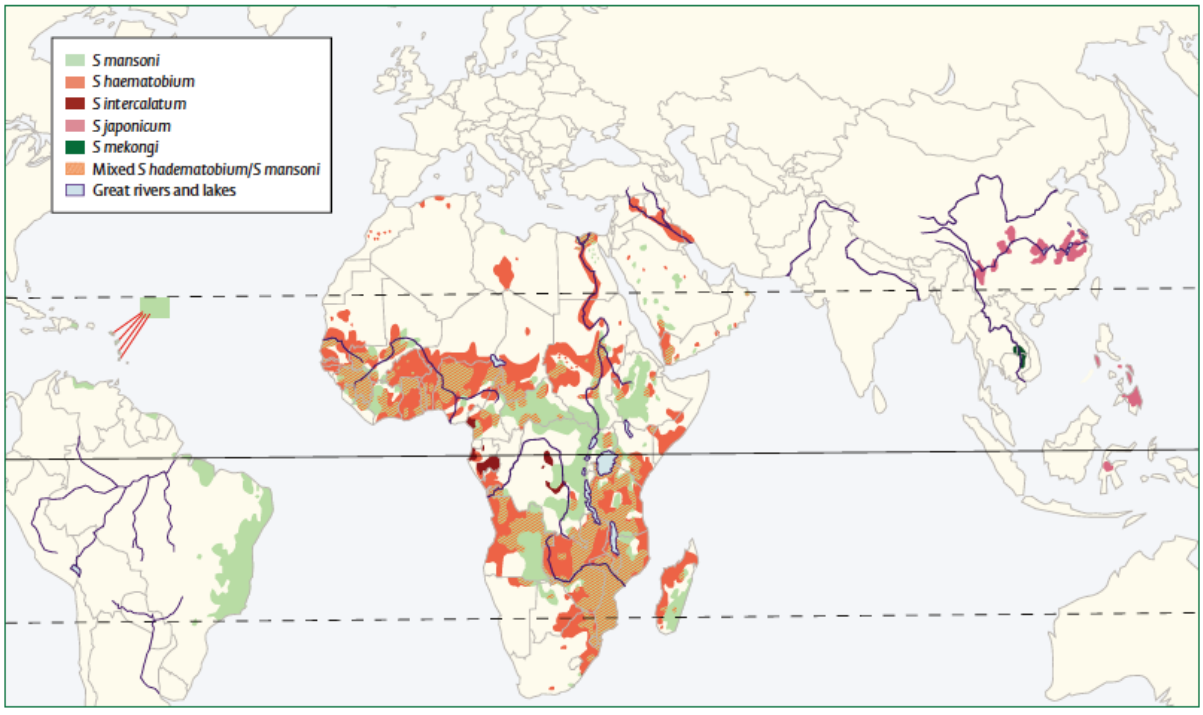

Figure 1. Global distribution of schistosomiasis-causing species (Gryseels *et al*., 2006).

The schistosome life cycle consists of two hosts: humans, the definitive host, and gastropods, the intermediate host (Figure 2). The life cycle begins when eggs are released with

feces or urine. The eggs hatch upon contact with water and release motile ciliated miracidia, which search for a suitable intermediate host. Snails of the genera *Biomphalaria*, *Oncomelania*, and *Bulinus* act as the intermediate hosts of *S. mansoni, S. japonicum,* and *S. haematobium*, respectively (Gryseels *et al.*, 2006). Upon finding a suitable host, the miracidia penetrate the snail tissue and multiply asexually to form multicellular sporocysts. The sporocysts mature into cercariae, and cercarial shedding is induced by light. Due to the asexual nature of cercariae production, one miracidium can give rise to thousands of cercariae, which can be released from the snail for months. Free-swimming cercariae, which can survive in the water for up to 72 hours, penetrate a vertebrate host, lose their characteristic bifurcated tail, and transform into schistosomulae. The schistosomulae migrate from the epidermal surface to the blood stream, where they enter the circulation. They migrate in the blood through the lungs and heart to eventually reach the portal blood vessels of the liver. It is here that the schistosomulae mature into adults and form mating pairs. The adult worm pairs migrate to the mesenteric veins of the intestine (*S. mansoni* and *S. japonicum*) or the bladder (*S. haematobium*), where they mate and deposit eggs (Gryseels *et al.,* 2006). Granuloma formation around the eggs enables their migration into the intestine or bladder (Hams *et al*., 2013; Pearce & MacDonald, 2002), where they are released with the feces or urine, respectively, and the cycle begins anew.

Adult worms measure 5-20 mm in length, with two terminal suckers at the anterior end (Figure 3a; Gryseels *et al.,* 2006). The worms have a simple, blind digestive tract and feed on host blood through anaerobic glycolysis, which primarily provides energy for male movement and female egg production (Gryseels, 2012). Following digestion, debris is regurgitated into the host's bloodstream (Gryseels *et al.,* 2006; Halton, 1997). Worm pairs remain in copula for

the duration of their lives (Figure 3b, LoVerde *et al*., 2004), which averages 3-5 years but can be up to 30 years (Gryseels *et al*., 2006).

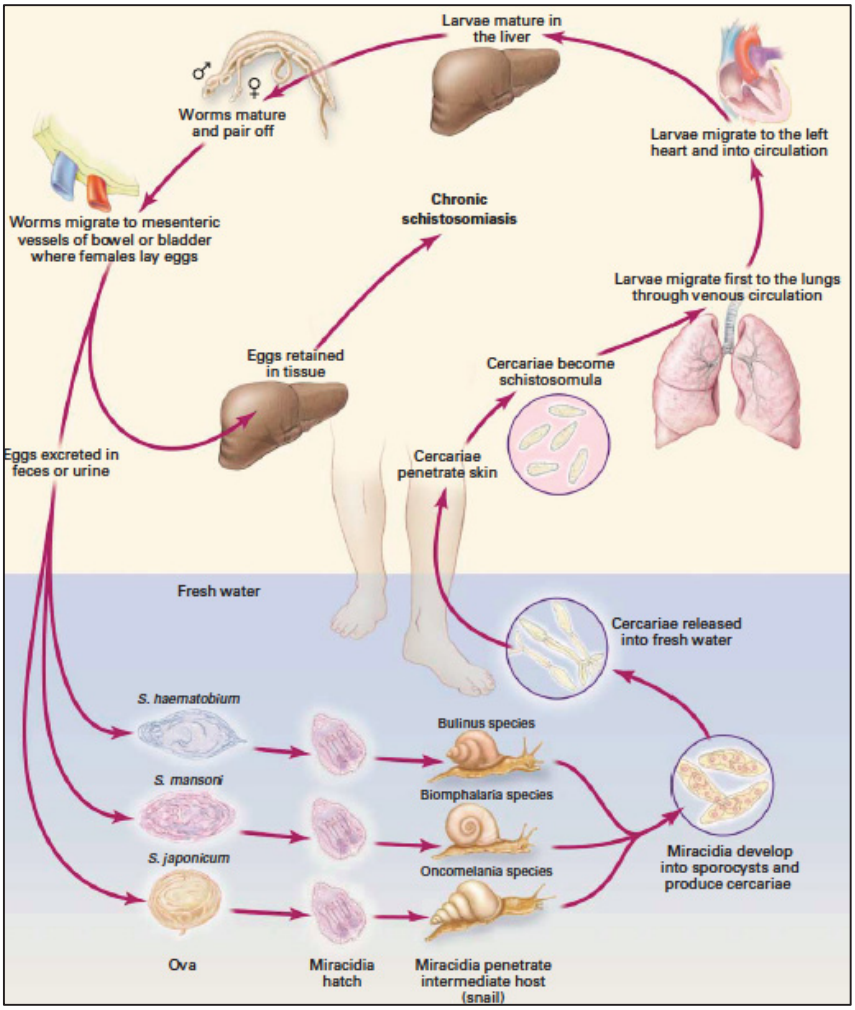

Figure 2: Schistosome life cycle (Ross *et al*., 2002).

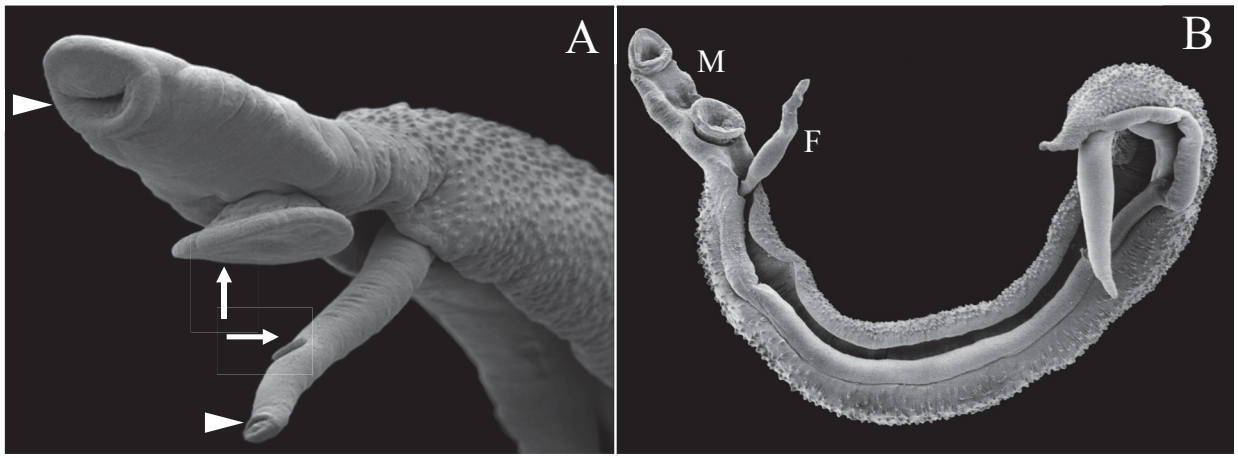

Figure 3: SEM images of adult schistosomes. A) Ventral and oral suckers of male and female worms. Arrows, ventral suckers; arrow heads, oral suckers (Adapted from Collins III & Newmark, 2013). B) Male and female worms in copula. M, male worm; F, female worm (Adapted from Natural History Museum, 2015)

1.2. Schistosomiasis

Almost 800 million people are at risk for schistosomiasis, and approximately 200 million people are infected, of whom 60 million are asymptomatic, 120 million are symptomatic, and 20 million present with severe disease (Chitsulo *et al*., 2000; Steinmann *et al*., 2006). The main diagnostic method, the Kato-Katz technique, detects eggs in the stool and urine but lacks sensitivity, particularly in low endemicity areas. Therefore, reported prevalence rates are thought to be an underestimate of the true number of infections. (de Vlas & Gryseels, 1992; Enk *et al*., 2008; Utzinger *et al*., 2011). Even though over 10% of the world's population is at risk, schistosomiasis is still classified as a neglected tropical disease, as direct mortality rates are low compared to diseases like HIV/AIDS, malaria, and tuberculosis (SCI, 2008). Schistosomiasis presents in two forms: acute or chronic.

Acute schistosomiasis, commonly referred to as Katayama fever, manifests a few weeks to months following primary infection and usually precedes appearance of eggs in feces and urine (Hams *et al*., 2013; Ross *et al*., 2012). This febrile illness is seen mainly in tourists and migrants (Ross *et al.,* 2002). An immune hypersensitivity reaction that results from migrating schistosomulae and egg deposition in tissues is to blame for this condition. Common symptoms include fever, fatigue, myalgia, malaise, and eosinophilia. Skin rash can also occur following cercarial penetration. Most affected people recover spontaneously after 2-10 weeks (Gryseels *et al*., 2006). Chronic schistsomiasis occurs as a result of egg embolization in tissues. Eggs that are not secreted remain in circulation and can become lodged in the liver and spleen (*S. mansoni* and *S. japonicum*) or genitourinary tract (*S. haematobium)*, and less frequently in the lungs or cerebrospinal system. Protease secretion by the eggs leads to an inflammatory reaction in the host, which triggers granuloma formation around the eggs (Figure 4a).

Granulomas are eventually replaced with fibrotic deposits (Figure 4b), which can lead to the obstruction of blood flow, resulting in portal hypertension, gastrointestinal varices, and hepatosplenomegaly following years of sustained heavy infection. Loss of appetite, abdominal pain, and bloody diarrhea are common symptoms of this disease (Gryseels *et al*., 2006; Hams *et al*., 2013; Pearce and MacDonald, 2002; Ross *et al*., 2002).

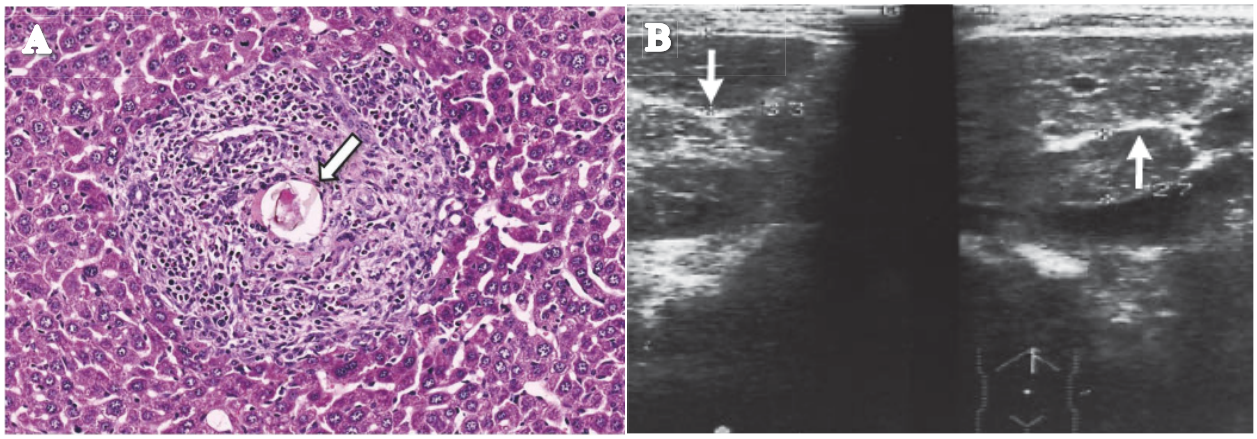

Figure 4. Schistosomiasis pathology. A). Granuloma formed around *S. mansoni* egg (arrow) in a mouse liver (Hams *et al*., 2013). B) Liver ultrasonogram showing fibrosis (arrows) in a man with severe hepatic schistosomiasis (Ross *et al*., 2002).

Schistosomiasis is most prevalent in sub-Saharan Africa, particularly in areas where access to clean water and healthcare is limited. The incidence of infection is highest in school-aged children, and its detrimental effects include impaired growth and development. The capacity for physical exertion in adults is reduced with chronic infection, leading to a loss of productivity. Schistosomiasis has also been associated with an increased risk of malnutrition and anaemia (Gryseels *et al*, 2006; King & Dangerfield-Cha, 2008). These damaging consequences leave those affected with a reduced ability to work, further promoting the cycle of poverty from which this disease has arisen (Utzinger *et al*., 2011).

1.3. Treatment and control

1.3.1. Praziquantel

Praziquantel (PZQ), an acylated quinoline-pyrazine compound that is active against all human schistosome species, is the only drug used on a large scale to treat schistosomiasis (Doenhoff *et al*., 2008; Gryseels *et al*., 2006). The anthelmintic activity of PZQ was observed initially at Bayer in the 1970s. It was originally used in veterinary medicine to treat various cestode and trematode infections (Andrews *et al*., 1983). The first human studies were conducted in 1978, and PZQ entered the market in the early 1980s (Cioli & Pica-Mattoccia, 2003; Olds & Dasarathy, 2000).

The mechanism of action of PZQ has not been elucidated, but it is thought that Ca^{2+} channels are the molecular target (Doenhoff *et al*., 2008; Greenburg, 2014). PZQ results in contractile paraylsis of the worm, which could be explained by large influxes of Ca^{2+} in the musculature (Cioli & Pica-Mattoccia, 2003; Doenhoff *et al.*, 2008, Greenburg, 2005; Pax *et al*., 1978). PZQ inhibits uptake of adenosine and uridine, nucleosides schistosomes are unable to synthesize *de novo*, which would directly affect worm survival. However, an antagonistic relationship between adenosine and Ca^{2+} channels has been demonstrated; therefore, blocking adenosine uptake and stimulating Ca^{2+} influx could be connected (Angelucci *et al*., 2007). PZQ also leads to morphological alterations in the worms. Vacuolization and blebbing of the tegument increases parasite antigen exposure, increasing susceptibility of worms to the host immune system. Therefore, worm clearance is dependent on a functional immune system, and PZQ efficacy is reduced in immunocompromised patients (Becker *et al*., 1980; Harnett & Kusel, 1986; Mehlhorn *et al*., 1981; Shaw & Erasmus, 1983).

PZQ cure rates have been reported to be greater than 60% after single dose treatments of 40 – 60 mg/kg; however, these rates are calculated based on egg release detected using the Kato-Katz technique, which as mentioned previously, lacks sensitvity. Therefore, actual cure rates could potentially be much lower (Doenhoff *et al*., 2008). PZQ is well-tolerated in most individuals. Mild and transient side effects that include headache, fever, dizziness, nausea, vomiting, abdominal pain, and diarrhea are seen in 30-60% of patients (Cioli *et al*., 2003; Gryseels *et al*., 2006). In addition to clearing infection of adult worms, administration of PZQ leads to regression of intestinal and vesical lesions, reactive hepatomegaly, and even mild liver fibrosis (Gryseels *et al*., 2006).

A problem of critical concern with PZQ is that it has little to no effect on immature worms (Doenhoff *et al*., 2008; Gryseels *et al*., 2006). Therefore, a second dose of PZQ is required approximately 4-6 weeks following initial administration. This can present a serious challenge in areas with high levels of transmission, as these areas are often the poorest and lack the necessary infrastructure and management for drug administration programs. Even in areas with adequate resources, compliance with drug administration programs is often less than ideal (Fenwick & Webster, 2006; Utzinger *et al*., 2011). One leading cause of low compliance, particularly in children, is the bitter taste of PZQ; vomiting and resistance to swallowing PZQ tablets was seen in children in Egypt (Fenwick *et al*., 2003).

Relying solely on the use of PZQ to treat schistosomiasis increases the threat of resistance development (Botros & Bennett, 2007; Doenhoff & Pica-Mattoccia, 2006; Fenwick & Webster, 2006). Resistant *S. mansoni* strains were isolated from Senegal and the Nile delta region of Egypt (Fallon *et al*, 1995; Ismail *et al*, 1996; Stelma *et al*., 1995; Tchuem Tchuente *et al*., 2001). *S. masoni* strains collected from patients treated in the Nile delta region had

ED_{50}s two to five times higher than eggs isolated before treatment (Ismail *et al*., 1996). However, in the field, repeated PZQ treatment resulted in eventual infection control, suggesting stable resistance was not established (Fallon, 1998). Lab isolates of *S. mansoni* have also been bred using selective pressure during mouse passages but were not stable in the absence of drug pressure (Cioli *et al*, 2004; Fallon & Doenhoff, 1994; Sabra & Botros, 2008). Merck KGaK is currently donating 250 million tablets of PZQ per year as part of mass drug administration (MDA) efforts to treat schistosomaisis, further increasing the chances of resistance developing as selection pressure increases.

1.3.2. Other anti-schistosomal drugs

Metrifonate and oxamniquine are alternative anti-schistosomal drugs but are only active against *S. haematobium* and *S. mansoni*, respectively (Utzinger *et al*., 2011). Oxamniquine also has more pronounced side-effects, including sleep induction and epileptic seizures. Artemisinin drugs have been shown to be effective in treating schistomiasis; however, administration of these drugs has been avoided in areas co-endemic with malaria due to the fear of resistance development in *Plasmodium* (Doenhoff *et al*., 2008; Gryseels *et al*., 2006). Meclonazepam, a benzodiazepine with schistosomicidal activity, cannot be used because it has severe sedative effects at therapeutically relevant doses (Doenhoff *et al*., 2008; Ribeiro & Geary, 2010).

1.3.3. Vector control

Eliminating the vector is another way of controlling parasite infections. For schistosomiasis, this involves eliminating the snail intermediate host. Attempting to reduce snail populations with molluscicides poses many problems. The chemicals are often toxic and

pose a threat to other inhabitants of the treated water bodies. Chemicals are also expensive, and areas with high levels of tranmission are often the poorest. Another method can involve introducing competitors or predators, which is even more logistically complex than molluscicide application. Efforts to reduce snail population are rarely successful in eliminating all snails; therefore, transmission can continue (Gryseels *et al*., 2006).

1.3.4. Successful control programs

Countries that have reduced schistosomiasis burdens to very low levels include Brazil, Burkina Faso, Cambodia, China, Egypt, Morocco, the Philippines, and Uganda (WHO, 2001; WHO, 2011). Integration of the two pillars of schistosomiasis control, treatment and targeting of the intermediate host, is key to reducing the prevalence of schistosomiasis, along with improving water sanitation and hygiene (Steinmann *et al*., 2006; WHO, 2011).

Although it is encouraging that there has been some success in reducing the impact of schistosomiasis, more political commitment is required by the governing bodies of these countries, along with increasing communication and coordination between said governments, organizations attempting to fight the disease, and the communitites targeted by the interventions, to achieve eradication (WHO, 2010).

More investment is being made to improve control efforts; however, there is still much to be done, including developing new drugs to treat schistosomiasis.

1.4. Schistosome nervous system

The schistosome nervous system is a promising target for therapeutic intervention. Schistosomes and other flatworms are acoelomates; therefore, endocrine signaling is not possible, and signal transduction in adults and developmental stages of the parasite is presumed

to rely on the nervous system. Vital parasite functions integrated and coordinated by the nervous system include host attachment and penetration, migration, feeding, excretion, and reproduction (Halton & Gustafsson, 1996; Ribeiro & Geary, 2010).

The nervous system of schistosomes consists of a central nervous system (CNS) and a peripheral nervous system (PNS). The CNS consists of a simple bilobed, ganglionic brain and paired ventral, lateral, and dorsal main nerve cords (MCs). The principal MCs run ventrally along the worm, reflecting the need for control of ventrally-located attachment organs and feeding aparatus, along with locomotion and copulation. These MCs are cross-linked at regular intervals by transverse ring commissures in a ladder-like configuration (Figure 5). CNS elements are linked to the PNS, which consists of a network of smaller nerve cords and plexuses (nerve nets) that innvervate the tegument, somatic musculature, suckers, alimentary tract and reproductive organs (Halton & Gustafsson, 1996; Halton & Maule, 2004; Ribeiro & Geary, 2010).

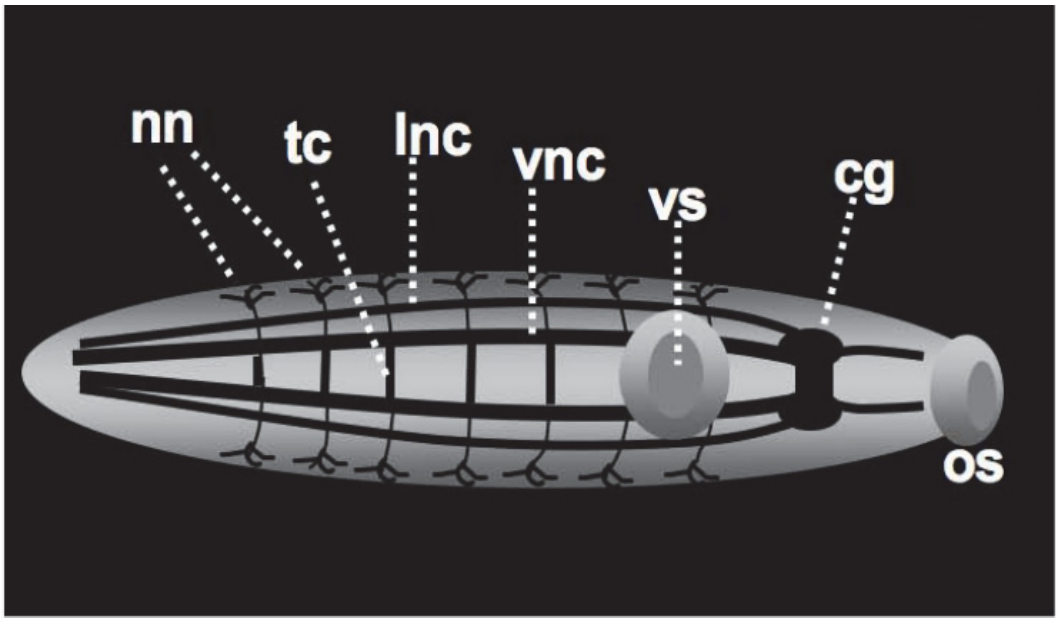

Figure 5. Key elements of the schistosome nervous system. Cg, cerebral ganglia; vnc, ventral nerve cord; lnc, lateral nerve cord; tc, transverse commissures; nn, nerve net; vs, ventral sucker; os, oral sucker (Patocka *et al*; 2014).

A vast array of neurotransmitters has been reported in schistosomes and they are thought to play important roles in signalling. The most abundant of these small "classical" transmitters are acetylcholine, biogenic animes (*i.e*., serotonin, histamine, norepinephrine, and dopamine), and glutamate (Bueding, 1952; Barker *et al.*, 1966; Halton & Maule, 2004; Hillman, 1983; Ribeiro & Geary, 2010; Tomosky *et al*, 1974). Neuropeptides and γ-aminobutyric acid (GABA) have also been identified as neurotransmitters in schistosomes (Halton & Maule, 2004; Mendonça-Silva *et al*., 2004).

1.5. Glutamate-gated chloride channels

Many anthelmintics target the neuromuscular system of parasitic worms (van den Eden, 2009). One very successful example is ivermectin (IVM), a macrocyclic lactone that targets glutamate-gated chloride channels (GluCls) in nematodes and arthropods. IVM is used widely in human and veterinary medicine to treat parasitic diseases such as onchocerciasis, or river blindness (*Oncocerca volvulus*), and lymphatic filariasis, or elephantiasis (*Wuchereria bancrofti*, *Brugia malayi*, and *Brugia timori*) in humans, heartworm disease (*Dirofilaria immitis*) in canines, and a wide range of gastrointestinal nematodes in livestock and companion animals (Cupp *et al*., 2011; Greenberg, 2014; Vercruysse & Rew, 2002).

GluCls are inhibitory ion channels: pore-forming membrane proteins that when bound by an agonist, allow chloride ions to difuse down their electrochemical gradient across the membrane, hyperpolarizing the cell (Changeux, 2010; Greenburg, 2014; Lynagh *et al*., 2015). GluCls are part of the pentameric ligand-gated ion channel (pLGIC) family, in which subunits are arranged in a five-fold symmetry (Figure 6; Thompson *et al*., 2010; Zemkova *et al*., 2014). Subunit composition can be homomeric or heteromeric, and each subunit consists of an

extracellular domain flanked by a signal peptide, where the ligand-binding pocket is located, and a carboxy-terminal transmembrane domain (TMD) with 4 membrane-spanning helices (M1-M4) (Lynagh & Lynch, 2012b; Thompson *et al*., 2010). The M2 helices are located centrally, forming the channel pore, and the amino acid composition of the M2 helices determines the ion selectivity of the chanel (Lynagh & Lynch, 2012b; Zemkova *et al*., 2014).

GluCls are found exclusively in invertebrates such as nematodes, insects, ticks, mites, mollusks, and crustaceans, and are closely related to vetebrate glycine- and GABA-gated channels (Greenburg, 2014; Wolstenholme, 2012; Zemkova *et al*., 2014). The functions of GluCls include control and modulation of locomotion, feeding, and the mediation of sensory input, among others (Greenburg, 2014; Wolstenholme, 2012).

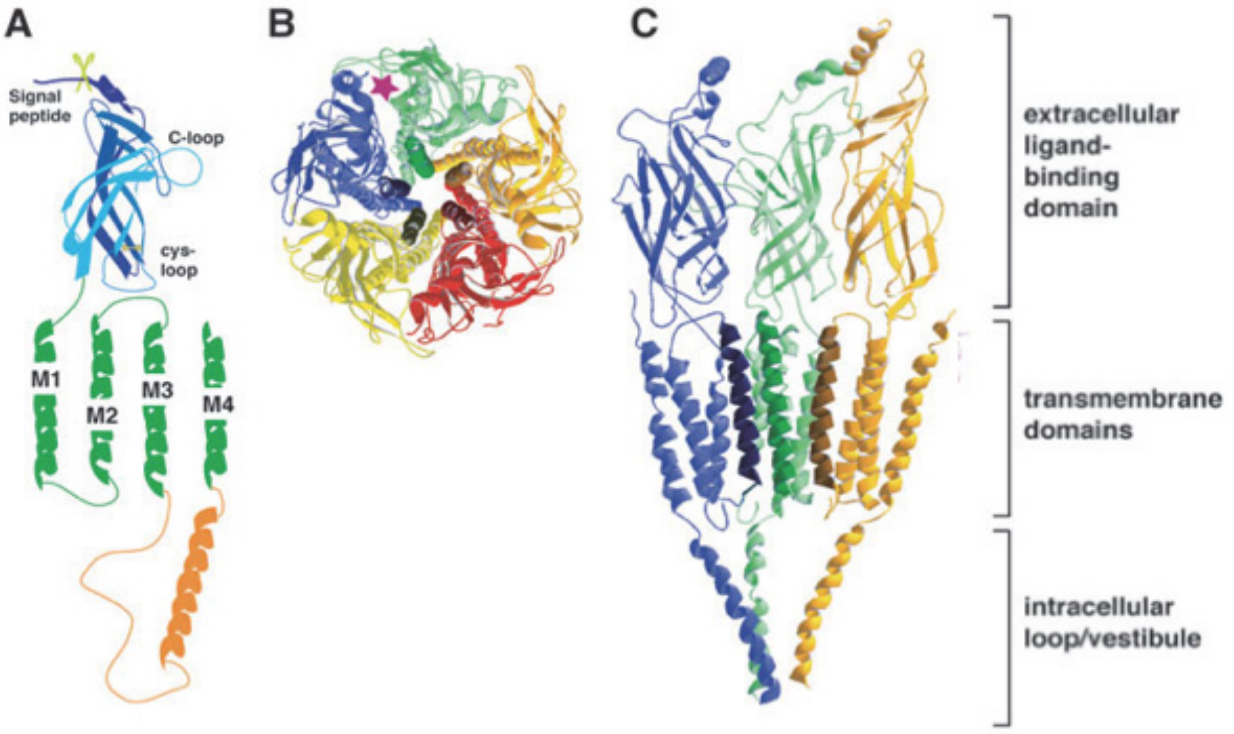

Figure 6. pLGIC structure. A) Cartoon representation showing topology of pLGIC subunit. B) Top view of a *Torpedo* nAChR, with each subunit a different colour and M2 helices darkened. Star, location of ligand-binding site. C) Side view with two subunits removed to reveal pore (Dent, 2010).

The release of the *S. mansoni* draft genome in 2009 by Berriman and colleagues and the subsequent high quality genome in 2012 by Protasio and colleagues led to the identification of 4 putative *S. mansoni* GluCls (SmGluCl-1, SmGluCl-2, SmGluCl-3, and SmGluCl-4; Berriman *et a.l*, 2009; Dufour *et al*., 2013; Protasio *et al.*, 2012). Full-length cDNAs were generated for 3 of the subunits (SmGluCl-1 to -3) with RACE experiments (Figure 7; Dufour *et al*., 2013). These 3 subunits were functionally characterized in *Xenopus laevis* oocytes. SmGluCl-2 and -3 formed functional homomeric glutamate receptors permeable to chloride ions when expressed individually, whereas SmGluCl-1 did not. However, SmGluCl-1 formed a heteromeric receptor responsive to glutamate when co-expressed with SmGluCl-2. All of the subunits were insensitive to IVM, either by direct activation or potentiation of glutamate response (Dufour *et al*., 2013). The TMDs of SmGluCls lack key molecular determinants for macrocyclic lactone binding. A glycine residue in M3 is substituted by a bulky residue in the schistosome GluCls, and M3-Gly, along with a proline in M1, are crucial for high IVM sensitivity. The electrophysiology experiments conducted by Dufour *et al.* corroborated the prediction that the glycine substitute in M3 would be sufficient to preclude IVM binding (Dufour *et al*., 2013; Lynagh & Lynch, 2010; Lynagh & Lynch, 2012a). The SmGluCls were also insensitive to 3-meclonazepam, suggesting that GluCls are not the likely target of schistosomicidal benzodiazepines (Dufour *et al*., 2013).

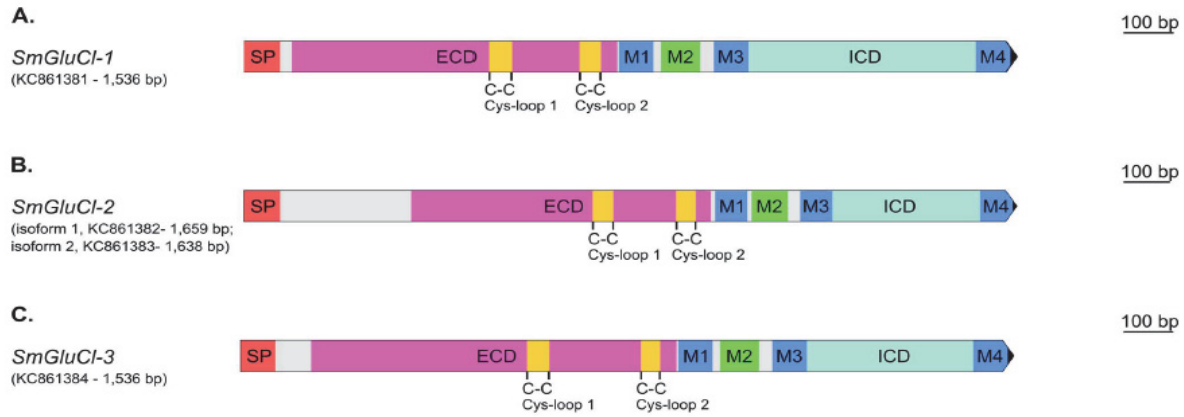

Figure 7. Gene structure of SmGluCls. A) SmGluCl-1 (Smp_096480). B) SmGluCl-2 (Smp_015630). C) SmGluCl-3 (Smp_104890). ECD, extracellular domain; ICD, intracellular domain; M1-4, membrane-spanning region 1-4; SP, signal peptide (Dufour *et al*., 2013).

Characterization of the fourth subunit, SmGluCl-4, is required to complete the story, which is the main focus of this thesis project. SmGluCl-4 is unusual in that it is approximately 1000 base pairs (bp) longer than the other 3 subunits (~2.6 kbp as compared to ~1.5 – 1.6 kbp; Figure 7 and Figure 8) (Dufour *et al*., 2013). SmGluCl-4 has most of the characteristic components of a pLGIC: an extracellular domain (ECD), an intracellular domain (ICD), membrane spanning regions (M1 – M4), and two Cys-loops. However, it lacks a signal peptide (SP), indicating that SmGluCl-4 may not be expressed at the cell surface in the parasite. Although SmGluCl-4 lacks a typical SP, reverse transcription polymerase chain reaction (RT-PCR) experiments showed that the gene encoding this subunit is transcribed in all human stages of the parasite, indicating that it may have an atypical SP not detectable with SignalP software (Center for Biological Sequence Analysis, Technical University of Denmark), or that it plays a different role (Dufour, 2013).

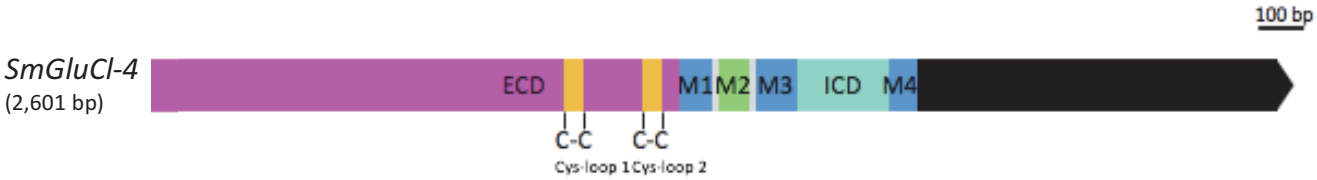

Figure 8. Gene structure of SmGluCl-4. ECD, extracellular domain; ICD, intracellular domain; M1-4, membrane-spanning region 1-4.

HYPOTHESIS

Knowing that SmGluCl-4 lacks a typical SP and is larger than the other SmGluCls, we hypothesize that SmGluCl-4 will not form functional homomeric or heteromeric glutamate receptors in *Xeonpus laevis* oocytes. However, due to the presence of SmGluCl-4 gene transcripts in all parasite stages, we hypothesize that SmGluCl-4 will be expressed throughout the parasite.

OBJECTIVES

This project has three main objectives:

1. Determine if SmGluCl-4 forms functional homomeric or heteromeric glutamate receptors using the *Xenopus laevis* expression system
2. Localize SmGluCl-4 in *Schistosoma mansoni* parasites using immunolabelling
3. Develop a fluorescence-based mammalian cell assay that could be scaled up to screen channel agonists/antagonists in a high-throughput screening setting. There is a need to identify potential agonists and agonists in order to study the roles of SmGluCls within the parasite.

CHAPTER II

METHODS AND EXPERIMENTAL APPROACHES

METHODS AND EXPERIMENTAL APPROACHES

2.1. Determining if SmGluCl-4 forms a functional glutamate receptor

2.1.1. *In vitro* transcription of capped RNA encoding SmGluCl-4

SmGluCl-4 was cloned into the ampicillin-resistance conferring bacterial plasmid pT7T7s, and pT7T7s was transformed into DH5α *Escherichia coli*. Stocks containing 50% glycerol were frozen at -80°C. Plasmid-containing DH5α was cultured in 5 ml Luria broth containing 0.1% ampicillin. Plasmids were extracted using the Z-10 Spin Column Plasmid DNA Minipreps Kit (Bio Basic Inc., Markham, Ontario). Plasmids were linearized with FastDigest XbaI (Thermo Scientific, Waltham, Massachusetts) for 30 min and purified using a GeneJET Gel Extraction Kit (Thermo Scientific). Capped RNA (cRNA) was synthesized *in vitro* using the mMessage mMachine T7 Transcription kit (Ambion, Burlington, Ontario). The transcription reaction was incubated at 37°C for 3-6 hr and cRNA was recovered by precipitation with LiCl. Capped RNA was resuspended in nuclease-free dH_2O and diluted to a final concentration of 1 ng/nl and stored at -80°C until use.

2.1.2. Expression of SmGluCl-4 in *Xenopus laevis* oocytes

To determine if SmGluCl-4 forms a functional homomeric channel, the subunit was expressed in *X. laevis* oocytes. Oocytes were injected with 40.6 ng (40.6 nl; 1 ng/nl) cRNA using the Nanoinject system (Drummond Scientific, Broomall, Pensylvannia) or 40.6 nl nuclease-free dH_2O (negative control) and incubated in ND96 (96 mM NaCl, 2 mM KCl, 1.8 mM $CaCl_2$, 1 mM $MgCl_2$, 5 mM Hepes, 2.5 mM sodium pyruvate, pH 7.3) at 19°C for 2 days.

Two-electrode voltage clamping (TEVC) was used to measure channel activity with oocytes clamped at -80 mV. Concentrations of L-glutamate (L-glu; dissolved in sodium-pyruvate-free ND96; Sigma-Aldrich, Oakville, Ontario) were applied to oocytes and responses were measured using AxoClamp 2B and Digidata 16-bit data acquisition system (Axon Instruments, Foster City, California) with Clampex 8.1 digital oscilloscope software (Axon Instruments). Data were analyzed using Clampfit 10.2 digital software (Axon Instruments). Decreases in current following agonist application indicate channel opening and influx of Cl^- ions. Responses were analyzed by monitoring the change in current upon L-glu application.

To determine if SmGluCl-4 forms a functional heteromeric channel with other subunits, the subunit cRNA was mixed separately with SmGluCl-1, -2, and -3 cRNAs at a ratio of 1:1 and injected into oocytes as detailed previously. Channel function was assessed as detailed previously, and concentration-response curves were produced using using Prism software (GraphPad, Version 6). To determine if functional heteromeric channels were formed, the EC_{50}s of the concentration response curves of combination-injected oocytes were compared to the EC_{50}s of oocytes expressing known functional homomeric channels.

2.2. Determining if SmGluCl-4 is expressed at the oocyte surface

Oocytes previously injected with SmGluCl-4 cRNA and SmGluCl-3 cNRA were fixed overnight in 4% paraformaldehyde (PFA; Sigma-Aldrich) at 4°C. Oocytes were washed three times with phosphate-buffered saline (PBS). Oocytes were incubated in primary antibody (rat anti-SmGluCl-4 diluted in AbD; GenScript, Piscataway, New Jersey) diluted in antibody diluent (AbD; 0.2% fish skin gelatin , 0.2% sodium azide and 0.1% Triton X-100 in PBS) (1:500 for SmGluCl-4 and 1:100 for SmGluCl-3) overnight at 4°C. Oocytes were washed three

times with AbD and then incubated in secondary antibody in AbD (Alexa Fluor® 488-conjugated goat anti-rat IgG; GenScript; 1:1000) overnight at 4°C. Oocytes were washed three times with AbD and another three times with PBS. A few drops of mounting media (Sigma-Aldrich) were added to a mounting chamber containing PBS. Oocytes were added along with a coverslip, and oocytes were examined using Bio-Rad Radiance 2100 confocal laser scanning microscope (Bio-Rad, Hercules, California) equipped with a Nikon Eclipse E800 fluorescence microscope (Nikon Instruments Inc., Melville, New York). The Alexa Fluor® 488 fluorescence was excited with the Argon laser (488 nm; HQ515/530 emission filter), and the oocytes were visualized using the 10X and 20X objectives.

2.3. Localizing SmGluCl-4 in adult *Schistosoma mansoni* using immunolabelling

2.3.1. Recovery of adult *S. mansoni* from infected mice

Dr. Paula Ribeiro provided adult *S. mansoni* for immunolocalization studies. Cercarial shedding was induced by exposing *S. mansoni*-infected *Biomphalaria glabrata* snails to light for 2 hr. Female CD1 mice were infected by tail exposure to ~250 cercariae/mouse for 1 hr. Adult worms were recovered by portal perfusion 6 weeks post-infection following euthanasia of mice by CO_2 inhalation. All work was performed in accordance with Dr. Ribeiro's animal care protocol (2001-3346).

2.3.2. Fixation and immunolabelling of adult *S. mansoni*

Male and female worms were separated and washed three times with PBS. Worms were then flat-fixed in 4% PFA for 4 hr at 4°C. Worms were washed three times with PBS and then

incubated three times with 0.1 M glycine (in PBS; Fisher Scientific) for 5 min at room temperature (RT). If worms were not used immediately, liquid was removed and samples were flash frozen in liquid nitrogen and stored at -80°C.

To permeabilize worms for immunolabelling, fixed worms were incubated in 1% SDS (in PBS) for 2 hr at RT. Worms were washed five times in AbD (0.1% bovine serum albumin (BSA; Sigma-Aldrich), 0.1% sodium azide, 0.5% Triton X-100 in PBS). Prior to addition of primary antibodies, worms were incubated in 1% BSA in AbD overnight at 4°C. Worms were incubated in primary antibody (rat anti-SmGluCl-4 diluted in AbD) for two days at 4°C. Worms were washed five times in AbD at 4°C. Worms were then incubated in secondary antibody (Alexa Flour 488-conjugated goat anti-rat IgG) for 2 days at 4°C. Rhodamine-conjugated phalloidin (Cytoskeleton, Inc., Denver, Colorado) was added along with the secondary antibody as a muscle counterstain. The worms underwent a final set of five washes in AbD at 4°C and were mounted in mounting media for examination using a Bio-Rad Radiance 2100 confocal laser scanning microscope equipped with a Nikon Eclipse E800 fluorescence. The Alexa Fluor® 488 fluorescence was excited with the Argon laser (488 nm; HQ515/30 emission filter), and the rhodamine fluorescence was excited with the Green HeNe laser (543 nm; HQ590/70 BLD emission filter). The worms were visualized using the 20X and 40X objectives.

Controls included the omission of primary antibody and replacement of primary antibody with peptide-adsorbed primary antibody.

2.4. Developing a mammalian cell assay to screen channel agonists/antagonists

2.4.1. Codon optimization of SmGluCl-2 for mammalian cell culture

SmGluCl-2 forms a functional homomeric glutamate receptor in *X. laevis* oocytes (Dufour *et al*., 2013) and was chosen as the construct for expression in a mammalian cell assay. SmGluCl-2 was modified by adding a sequence codon-optimized for expression in mammalian cells and by adding a DYKDDDDK flag for epitope detection by immunofluorescence. The modified SmGluCl-2 construct was cloned into the pCU57 vector. PCU57-SmGluCl-2-flag was synthesized by GenScript. SmGluCl-2-flag was digested out of pCU57 and inserted into the mammalian vector pCI-neo (Promega, Madison, Wisconsin). PCI-neo was transformed into DH5α *E. coli*. Stocks containing 50% glycerol were frozen at -80°C. Plasmid for transfection was extracted as described in section 2.1.1.

2.4.2. Transfection of HEK 293F cells with SmGluCl-2-flag and YFP

Human embryonic kidney (HEK) 293F cells (ATCC, Manassas, Virginia) were cultured in Dulbecco's modified Eagle's medium (DMEM; Gibco, Waltham, Massachusetts) supplemented with 10% heat-inactivated fetal bovine serum (FBS) (Invitrogen, Waltham, Massachusetts). Cells were cultured in a 37°C, 5% CO_2 incubator and were passaged every 2-3 days. Twenty-four hours prior to transfection, cells were seeded at density of 200,000 cells/well in a 6-well dish. Cells were transiently transfected with pCI-neo-SmGluCl-2-flag and pCDNA3.1-YFP (Addgene, Cambridge, Massachusetts) using the X-tremeGENE 9 DNA transfection reagent (Roche, Mississauga, Ontario) following the manufacturer's instructions. Controls included cells mock-transfected with pCI-neo and YFP.

Twenty-four hours post-transfection, cells were harvested using 0.25% trypsin (Thermo Scientific) and the trypsin was inactivated by adding DMEM containing FBS. Cells were washed twice with 2 mM EDTA in PBS and once in PBS to reduce cell clumping. Cells were then resuspended in FBS-free Fluorobrite DMEM (Gibco) and seeded at a density of 100,000 cells/well in a poly-L-lysine-coated, flat-bottomed, black-walled 96-well plate (Corning, Waltham, Massachusetts). Cells were incubated at 37°C for ~3 hr to allow adherence of cells to the bottom of the wells.

2.4.3. Confirmation of protein expression

To confirm transcription and expression of SmGluCl-2-flag, cells were seeded for transfection on sterile coverslips placed inside a 6-well dish. Twenty-four hours following seeding, cells were transfected as described in the previous section. Twenty-four hours post-transfection, the cells were washed very gently with PBS and were then fixed in 4% PFA for 15 min at RT. Cells were washed three times with PBS and then incubated with 0.1 M glycine in PBS three times for 5 min at RT. Cells were briefly treated with 0.1% Triton X-100 for 45 sec and washed again three times with PBS. Prior to addition of primary antibody, cells were incubated in 1% BSA in PBS (blocking buffer) for 30 min. Cells were incubated with primary monoclonal anti-FLAG antibody (Mouse anti-flag M2 IgG_1, Sigma-Aldrich) in blocking buffer for 1 hr at RT. Cells were washed three times with PBS and then incubated with secondary antibody in blocking buffer (Alexa Flour 488-conjugated goat anti-mouse IgG; Invitrogen) for 30 min at RT. DAPI (Sigma-Aldrich) was added during the final 5 minutes of secondary antibody incubation. Cells were then washed three times with PBS and then mounted on a slide with a drop of mounting media. Slides were then examined using using a Bio-Rad Radiance

2100 confocal laser scanning microscope equipped with a Nikon Eclipse E800 fluorescence. The Alexa Fluor® 488 fluorescence was excited with the Argon laser (488 nm; HQ515/30 emission filter), and the DAPI fluorescence was excited with the Blue Diode laser (505 nm; HQ442/45 emission filter). The cells were visualized using the 40X objective and 60X objective with oil.

To confirm transcription and expression of YFP, fixing and antibody-tagging were not required as YFP is a fluorescent protein. Cells were instead visualized using an Nikon Eclipse TE2000-U microscope using the 10X and 20X objectives (Nikon Instruments Inc., Melville, New York). The cells were transfected and seeded as described in the previous section. YFP expression was then assessed using a FITC filter and images were captured using a Hamamatsu Orca-ER digital camera (Hamamatsu City, Japan).

2.4.4. Detection of channel activity

To determine the optimal excitation and emission wavelengths for detection of YFP fluorescence, multiple settings were assessed using a Synergy H4 plate reader (Bio Tek Instruments, Inc., Winooski, Vermont). The optimal conditions were determined to be 500 nm excitation and 530 nm emission.

Sodium iodide (NaI; Sigma-Aldrich) was added to the cells as iodide acts as a surrogate ion for chloride in this assay. Upon channel activation, iodide ions enter the cells and interact with YFP, thereby quenching fluorescence. NaI was added to cells at final concentrations of 25 mM, and cells were incubated at 37°C for 30 min. Fluorescence levels were assessed prior to the addition of NaI and following incubation using a Synergy H4 plate reader (BioTek, Winooski, Vermont). The machine was maintained at 37°C, and bottom endpoint readings

were taken. Five microliters of L-glu (dissolved in PBS) was added to cells at final concentrations of 25 μM to determine. PBS was used as a no-drug control. Fluorescence readings were taken prior to addition of agonist and continued post-application. The agonist effect was calculated by determining the change in YFP fluorescence pre- and post-addition of agonist in comparison to no-drug controls using Prism software.

CHAPTER III

RESULTS

RESULTS

3.1. Electrophysiological characterization

3.1.1. Testing homomeric channel formation

We were unable to detect response to L-glu application in *Xenopus laevis* oocytes injected with SmGluCl-4 cRNA, suggesting that SmGluCl-4 does not form a functional glutamate receptor. TEVC experiments were performed on oocytes injected with cRNA encoding SmGluCl-4. Concentrations of L-glu (0.1 µM – 1000 µM) were applied to the oocytes, and no detectable response was seen in those injected with SmGluCl-4, as compared to positive control oocytes (SmGluCl-3-injected) (Figure 9).

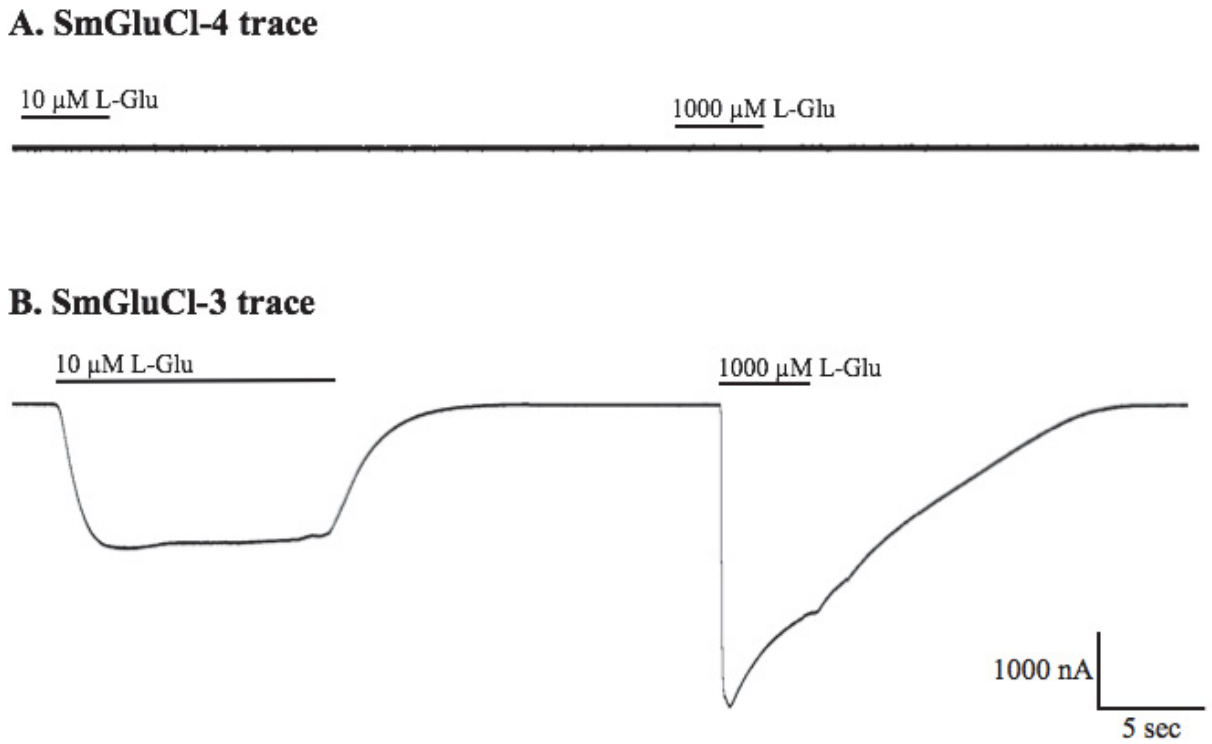

Figure 9. Electrophysiology traces from two-electrode voltage clamp experiments testing SmGluCl-4 channel formation. *Xenopus laevis* oocytes were injected with *in vitro* transcribed SmGluCl-4 or SmGluCl-3 capped RNA. TEVC experiments were performed and varying concentrations of L-glutamate were applied (10 µM and 1000 µM shown here). A. SmGluCl-4-injected oocytes did not respond L-glu. B. Positive control SmGluCl-3-injected oocytes responded robustly to L-glu. Decrease in current (nA) indicates channel activity. The bar above the trace indicates the period of L-glu application.

3.1.2. Localizing proteins at oocyte surface

Oocytes injected with SmGluCl-4 cRNA that were confirmed electrophysiologically to be insensitive to L-glu were fixed and probed with SmGluCl-4 specific antibodies. Confocal examination showed that SmGluCl-4 is expressed at the oocyte surface, indicating that lack of L-glu response in SmGluCl-4 oocytes was not due to lack of protein expression at the oocyte surface (Figure 10a). SmGluCl-3-injected oocytes probed with SmGluCl-3-specific antibodies were used as positive controls as they were shown to respond to L-glu, which would require protein expression at the oocyte surface (Figure 10b). No surface localization was seen in water-injected oocytes probed with SmGluCl-4 antibodies, indicating that there are no non-specific interactions with the primary antibody and the oocyte surface (Figure 10c). There was also no signal when primary antibody was omitted with SmGluCl-4-injected oocytes, indicating that the secondary antibody does not bind non-specifically to any oocyte epitopes (Figure 10d).

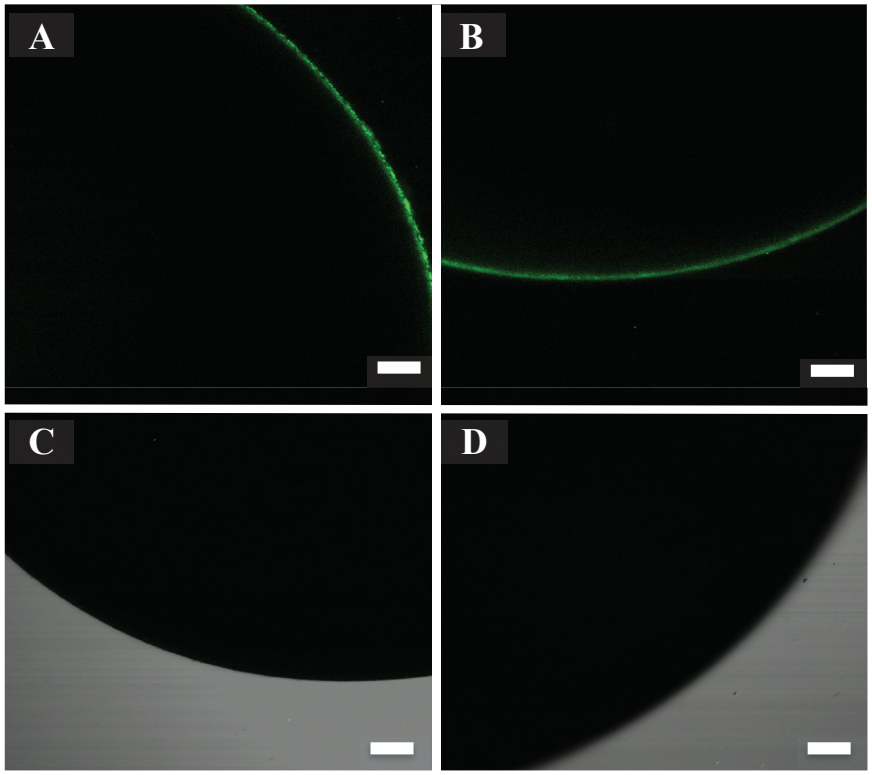

Figure 10. Antibody-probed oocytes visualized with confocal microscopy. A. SmGluCl-4-injected oocytes probed with anti-SmGluCl-4 antibodies. Fluorescence image only. B. SmGluCl-3-injected oocytes probed with anti-SmGluCl-3 antibodies. Fluorescence image only. Green signal indicates specific antibody binding to an epitope at oocyte surface. C. Water-injected oocytes probed with anti-SmGluCl-4 antibodies. Fluorescence image merged with transmission image to aid in visualization of oocyte membrane. D. SmGluCl-4-injected oocytes probed with secondary antibody only. Fluorescence image merged with transmission image as in C. Scale bar = 50 μM.

3.1.3. Testing heteromeric channel formation

When co-expressed with other subunits (SmGluCl-1 – 3) at a 1:1 ratio, SmGluCl-4 did not form a functional heteromeric glutamate receptor. No change in current was seen when varying concentrations of L-glu was applied to oocytes co-injected with SmGluCl-4 and SmGluCl-1, indicating that no channel formed. This is not surprising as neither subunit forms a functional homomeric receptor when when expressed individually.

To determine if SmGluCl-4 forms a heteromeric channel with either of the other two subunits, concentration-responses to L-glu were assessed. Response curves of the individually-injected oocytes were compared to that of the combination-injected oocytes, and it is assumed that a shift in response to L-glu is representative of a different pharmacological profile, hence heteromeric (containing SmGluCl-4) channel formation. When co-expressed with SmGluCl-2, the results do not support heteromeric channel formation. The concentration-response curves show nearly identical relationships between the individual SmGluCl-2 response as compared to SmGluCl-2 and -4 (Figure 11a). The EC_{50} for SmGluCl-2 receptors is 12.01 ± 0.84 μM (n = 15; EC_{50} = mean ± SE) and the EC_{50} for SmGluCl-2 in combination with SmGluCl-4 is 11.04 ± 0.50 μM (n = 16) ($P > 0.05$, paired T-test). The results also do not support heteromeric channel formation between SmGluCl-3 and SmGluCl-4 (Figure 11b). There is more variability in the concentration-responses of individually tested oocytes in this case; however, the EC_{50}s (SmGluCl-3 = 5.93 ± 0.89 μM, n = 15; SmGluCl-3:SmGluCl-4 = 7.37 ± 1.50 μM, n = 16) are still not significantly different ($P > 0.05$, paired T-test).

It is possible that heteromeric channels are forming and have the same pharmacological profile as their homomeric counterpart (i.e., SmGluCl-2:SmGluCl-4-injected oocytes and

SmGluCl-2-injected oocytes respond in the same manner to L-glu); however, these methods do not allow us to differentiate between the two populations.

Although SmGluCl-4 does not form either functional homomeric or heteromeric glutamate receptors, the electrophysiology experiments in this thesis have shown that results obtained using this system are reproducible. Previously published work by Dufour *et al*., showed the EC_{50}s of SmGluCl-2 and SmGluCl-3 receptors to be 11.77 ± 0.60 µM and 6.97 ± 0.45 µM, respectively (Dufour *et al*., 2013), as compared to the EC_{50}s determined in the current experiments, 12.01 ± 0.84 µM and 5.93 ± 0.89 µM, respectively.

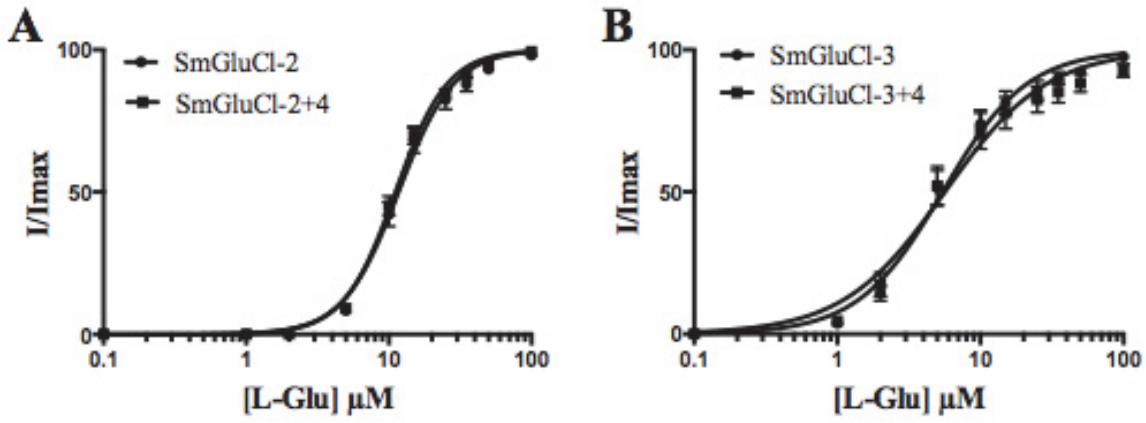

Figure 11. L-glutamate concentration-response curves of oocytes injected with single and combination cRNA. A. Concentration-response curves of oocytes injected with SmGluCl-2 alone vs SmGluCl-2:SmGluCl-4. B. Concentration-response curves of oocytes injected with SmGluCl-3 alone vs SmGluCl-3:SmGluCl-4. [L-glu] is L-glutamate concentration. Individual oocyte responses were normalized to their maximal response to L-glu (I/Imax). N = 3 (where N is number of times the experiment was repeated with different oocytes) and n ≥ 15 (where n = number of oocytes). Error bars represent SEM.

3.2. Subunit immunolocalization

3.2.1. Localizing SmGluCl-4 in adult parasites

Immunolocalization studies in adult worms showed that SmGluCl-4 is found throughout the nervous system of male and female worms. Strong immunofluorescence signals were seen

in the cerebral ganglia and longitudinal nerve cords in females (Figure 12) and in the cerebral ganglia, main commissure and nerve cords emanating from the head in males (Figure 13).

Some labelling of the longitudinal nerve cords is seen in both male and female worms; however, localization in the body of the adults was difficult. Multiple attempts yielded few results. To determine if lack of SmGluCl-4-labelling was due to lack of SmGluCl-4 expression, worms were simultaneously probed with anti-SmGluCl-3 antibodies, which have previously been shown to localize to the nerve nets, sub-tegumental nerve plexus, and tubercles in males (Dufour, 2013). No SmGluCl-3 labelling was seen, indicating the lack of SmGluCl-4 labelling may be due to a problem with the procedure.

Phalloidin staining (red) allows for visualization of muscle and structural identification within the worms. Phalloidin fluorescence intensity was strong throughout the body of the adult worms; however, phalloidin labelling was sometimes weak in the head region, especially in females, which could be explained by the reduced levels of muscle in the anterior end. Overlays of phalloidin fluorescence and SmGluCl-4 fluorescence showed no co-localization, indicating that SmGluCl-4 is not found in neuromuscular junctions.

Negative controls, which included worms probed with secondary antibody only, and worms probed with antibodies pre-adsorbed with the peptide antigen, showed some levels of non-specific binding (Appendix, Figure A1). However, no discernable specific binding was seen, allowing us to conclude that the patterns seen in worms probed with anti-SmGluCl-4 antibody are attributable to the expression of this protein within the adult.

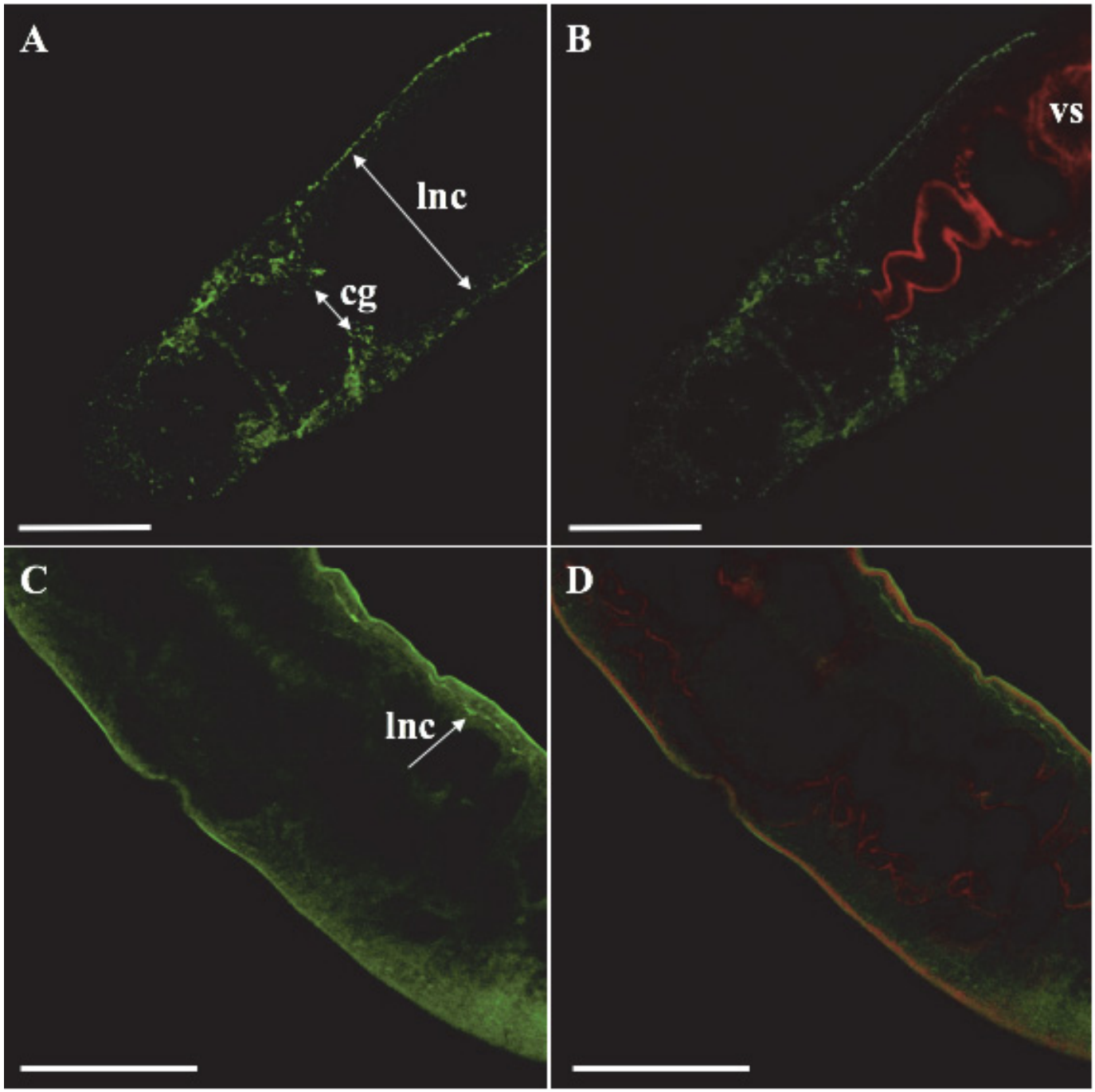

Figure 12. Tissue localization of SmGluCl-4 in *Schistosoma mansoni* adult females. Confocal microscopy images (Z-stacks) of *S. masoni* females probed with rat anti-SmGluCl-4 primary antibody and AF-488 goat anti-rat secondary antibody (green), counterstained with rhodamine-phalloidin. A. SmGluCl-4 is localized throughout anterior end of the female. C. SmGluCl-4 is found in lateral nerve cords in the female body. B, D. Overlays with phalloidin shows no apparent co-localization. cg, cerebral ganglia; lnc, lateral nerve cord(s); vs, ventral sucker. Scale bar = 50 μM.

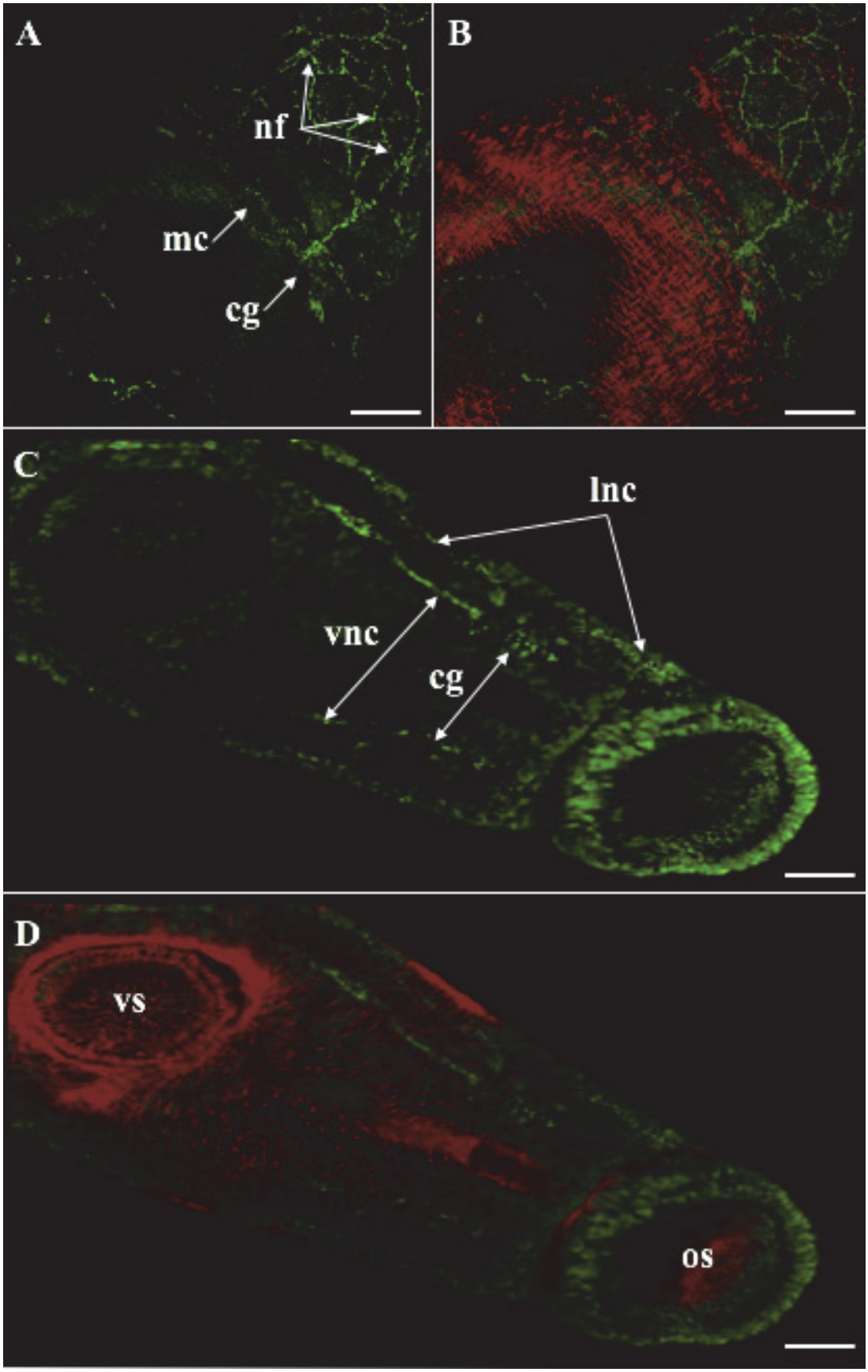

Figure 13. Tissue localization of SmGluCl-4 in *Schistosoma mansoni* adult males. Confocal microscopy images (Z-stacks) of *S. masoni* males probed with rat anti-SmGluCl-4 primary antibody and AF-488 goat anti-rat secondary antibody (green), counterstained with rhodamine-phalloidin. A, C. Strong SmGluCl-4 signal are seen throughout anterior end of the male. B, D. Overlays with phalloidin shows no apparent co-localization. cg, cerebral ganglia; nf, nerve fibers; lnc, lateral nerve cord(s); mc, main nerve cord; os, oral sucker; vnc, ventral nerve cords; vs, ventral sucker. Scale bar = 50 μM.

3.3. Mammalian cell assay development

3.3.1. SmGluCl-2-flag transfection in HEK 293 cells

Following transfection into HEK 293 using the X-tremeGENE 9 DNA transfection reagent from Roche, SmGluCl-2-flag is expression is very low. Immunolocalization shows that SmGluCl-2-flag is expressed at the surface of some cells; however, the transfection efficiency is very low (<10% cells), indicating that optimization of the transfection procedure is required to proceed with assay development.

3.3.2. YFP transfection in HEK 293 cells

Following transfection into HEK 293 cells, YFP is transcribed and highly expressed as seen in Figure 14. This level of fluorescence indicates that transfection efficiency is high and optimization of transfection conditions for YFP were successful. Cells were seeded and transfected at varying densities, and different YFP-plasmid stocks were tested and transfected, while varying the ratio of transfection reagent to DNA. Transfection efficiency may change while optimization of transfection conditions continues for SmGluCl-2-flag (the plasmids are co-transfected); however, YFP transfection appears robust and will hopefully remain at levels easily detectable by a plate reader.

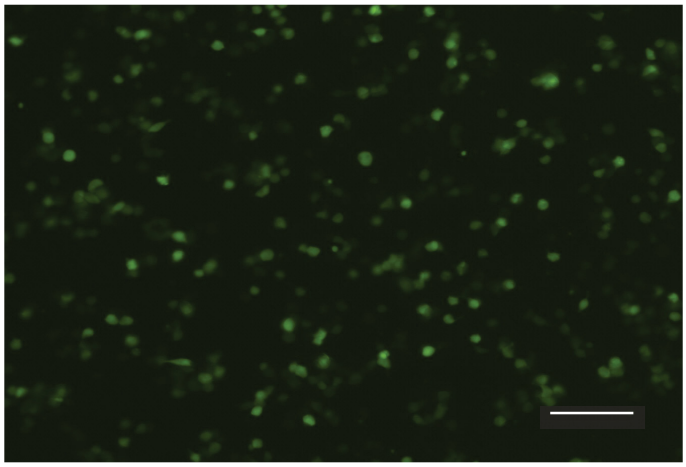

Figure 14. Expression of transfected YFP in HEK 293 cells. HEK 293 cells were transiently transfected with YFP and visualized using a FITC filter on a Nikon Eclipse TE2000-U inverted fluorescence microscope. Scale bar = 100 μM.

CHAPTER IV

DISCUSSION

DISCUSSION

Schistosomiasis affects some of the most disadvantaged people in the world. Two hundred million people are infected and close to 800 million people are at risk, with a death toll nearing 200,000 people annually (Chitsulo *et al*., 2000; Steinmann *et al*., 2006). Like most parasitic infections, there is no vaccine available, and currently only one drug, PZQ, is used to treat schistosomiasis (Doenhoff *et al*., 2008; Gryseels *et al*., 2006). The threat of resistance development looms with the use of a single drug, and pressure is increasing with the boost in supply of PZQ for MDA programs. Furthermore, PZQ is not effective against the juvenile stage of the parasite (Doenhoff *et al*., 2008; Gryseels *et al*., 2006). Therefore, there is a great need for a new anthelmintic to treat schistosomiasis.

The nervous system of schistosomes is an attractive target for drug development as it coordinates many vital parasite functions. GluCls are of particular interest as they have been successfully targeted in nematodes and insects (i.e., the macrocyclic lactone IVM), and have been recently identified in schistosomes (Dufour *et al*., 2013). Three *S. mansoni* GluCls (SmGluCl-1 – 3) were characterized previously. The subunits were expressed in *Xenopus laevis* oocytes and were tested for glutamate sensitivity using electrophysiology (Dufour *et al*., 2013). SmGluCl-2 and SmGluCl-3 formed functional homomeric channels when expressed individually and SmGluCl-1 forms a functional heteromeric channel when co-expressed with SmGluCl-2 (Dufour *et al*., 2013). The subunits were also characterized by immunolocalization within the parasites. Nervous system localization was seen with all the subunits (Dufour, 2013). Study of the fourth subunit was required for completion of basic knowledge of these

flatworm GluCls, and work in this thesis involved characterizing SmGluCl-4 using the same methods as outlined above.

Electrophysiological characterization of SmGluCl-4 showed that the subunit does not form a functional homomeric receptor sensitive to L-glu, nor does it form a functional heteromeric receptor when co-expressed with any of the subunits. However; immunolocalization studies with oocytes injected with SmGluCl-4 cRNA showed subunit expression at the surface. It is possible that SmGluCl-4 forms a channel *in vivo* and that the heterologous oocyte system does not allow expression of a functional protein. Chaperone or accessory proteins may be required for proper assembly of the pentameric form. Accessory proteins are required for proper assembly of some nematode receptors in oocytes (Boulin *et al*., 2008; Boulin *et al*., 2011, Duguet *et al*., 2016). Unfortunately, due to the very recent identification of the SmGluCls, nothing is known about flatworm accessory proteins.

It is possible that, even though the protein has been shuttled to the surface, it is not folded properly. This could be due to its increased size – it is approximately 1000 bp longer than the other three subunits. Even if the SmGluCl-4 subunits themselves are assembled properly, the longer C-terminal tail could interfere with assembly into the pentamer. It is possible that this C-terminal tail is somehow modified post-translationally in the worms, thereby removing this problem. Attempts to extract parasite protein and test this on a Western blot were not successful, as SmGluCl protein concentration was not sufficient. It is also possible that SmGluCl-4 acts as a regulatory protein and simply no longer forms a functional glutamate receptor, which would explain its expression in the worm but lack of response to glutamate in oocytes.

When determining which assay type to use when developing a high-throughput screen, there are many considerations. Patch-clamp electrophysiology is considered the "gold-standard," as it can detect single-channel currents. However, even with recent developments in automated patch-clamp systems, the process is still laborious, requires stable cell lines, and is relatively low-throughput (Harrison *et al*., 2014; Polonchuk, 2012; Wang and Li, 2003). Membrane potential assays are also very sensitive, but require dye-loading steps and incubations, and they are relatively expensive (Fitch *et al*., 2003). A YFP based assay was chosen, as they have been developed previously for high-throughput screening and do not require stable transfectants (Galietta *et al*., 2001a; Galietta *et al*., 2001b; Gilbert *et al*., 2009; Kruger *et al*., 2005; Sui *et al*., 2010). Mutations to the original YFP protein have increased the sensitivity to halide ions and the levels of fluorescence produced, making YFP a very good indicator in fluorescence-based anion channel assays (Galietta *et al*, 2001a; Jayaraman *et al*., 2000). Quenching of YFP is fast, robust, and proportional to channel activation; fold-change in YFP fluorescence can be directly correlated to chloride channel activity. Transfection of YFP also drastically reduces the costs and processing time that would be incurred when using a baculovirus delivery system, such as the one from Molecular Probes used by MacDonald *et al*. (2014). Preliminary assays showed fluorescence reduction in response to L-glu application; however, optimization is required before the assay can be scaled up for high-throughput screening.

Ideally we would have a stable cell line that would express both SmGluCl-2 and YFP; however, previous attempts to generate a stable cell line with SmGluCl-2 were not successful. It was proposed that high levels of expression of SmGluCl-2 are toxic to the cells. A study by Ye and Sontheimer (1998) examined the glutamate levels in multiple FBS samples and

determined the concentration to be around 1 mM. When the FBS is diluted with growth media to make complete media, the L-glu concentration is still likely to be around 100 μM, a concentration more than 8-fold higher than the EC_{50} for SmGluCl-2 in oocytes; continuous exposure to glutamate could cause SmGluGl-2 desensitisation. This could lead to a disruption in chloride ion balance, which could lead to cell death. To avoid this effect, media glutamate levels could be reduced by supplementation with either glutamate dehydrogenase or glutamate decarboxylase, which convert L-glu to α-ketoglutarate and GABA, respectively (Brosnan and Brosnan, 2013; Sonnewald *et al*., 1997). Alternatively, SmGluCl-2 could be incorporated into an inducible system like the Tet-On system, where the expression of SmGluCl-2 could be induced by addition of tetracycline or its derivative doxycycline before beginning the assay (Hoppe *et al*., 2014; Shaikh and Nicholson, 2006). However, this system would require the stable selection of three plasmids: the regulatory plasmid, the response plasmid (encoding SmGluCl-2), and the YFP plasmid.

FUTURE DIRECTIONS

Although neither functional homomeric nor heteromeric glutamate receptors form when SmGluCl-4 is expressed in the heterologous oocyte system, immunolocalization studies showed that SmGluCl-4 was expressed throughout the nervous system of the adult parasite, indicating that it may play some physiological role. Future work could involve investigating this potential role of SmGluCl-4 within the parasite using RNA interference (RNAi). RNAi would allow us to specifically knock down the SmGluCl-4 gene in parasites *in vitro* and study the effects on the worms (Agrawal *et al*., 2003). It would also be interesting to conduct RNAi experiments with the other 3 subunits to determine their roles within the worms. Additionally,

the RNAi experiments could be done with the cercarial stage and correlated with expression levels at the different stages using qPCR.

The preliminary results of the cell assay showed that the reduction in fluorescence upon application of L-glu in SmGluCl-2 and YFP-transfected cells and mock-transfected (pCI-neo and YFP) differ significantly ($p > 0.005$; One-way ANOVA comparing all samples) (Figure 15). However, the experiment was only performed once, and more work is required to increase transfection efficiency of SmGluCl-2. Before beginning optimization of SmGluCl-2 transfection, it might be worthwhile to switch cells lines from HEK 293 to a more adherent cell line. For example, HEK 293 cells are easily dislodged from the bottom of a plate upon application of slight physical pressure (e.g., when NaI is added before the start of the assay), forcing us to coat the assay plates in poly-L-lysine before seeding the cells. This step adds upwards of two hours to the processing, as the plate has to be coated, washed multiple times, and dried completely before the cells can be seeded. In contrast, baby hamster kidney (BHK 21) and Chinese hamster ovary (CHO) cells are very adherent and would eliminate the need for the plate-coating step (Omasa *et al*., 2010; Stoker and MacPherson, 1964). The transfection should still be successful, as BHK 21 and CHO are mammalian cell lines, and the SmGluCl-2 and YFP genes are encoded in plasmids with mammalian promoters. After establishing optimal transfection conditions for both SmGluCl-2 and YFP, optimization for HTS could be continued as detailed below.

The optimal concentration of L-glu will be determined by applying a range of L-glu concentrations and creating a concentration-response curve, from which we can determine the EC_{50}. The L-glu concentration that approximates the EC_{50} will then be used in HTS assays to determine the effects of modulators (i.e., agonists and antagonists) on SmGluCl-2 activity, a

method used previously to assess the activities of nicotinic acetylcholine and GABA receptors in mammalian cells (Liu *et al*., 2008; Nashmi *et al*., 2003). To ensure homogeneity of SmGluCl-2 expression, transiently transfected cells could be cryopreserved for future use (Johansson *et al*., 2013; Liu *et al*., 2008). Alternatively, attempts could be made to establish a stable cell line expressing both SmGluCl-2 and YFP as discussed previously

Following HTS optimization, compounds obtained from the Broad Institute (Cambridge, Massachusetts), and microbial fermentation extracts from the Merk collection at the Natural Products Discovery Institute (Doylestown, Pennsylvania) will be tested at the McGill HTS Facility (Montreal, Quebec). Compounds that cause a significant increase or decrease in SmGluCl-2 activity could be tested on the worms *in vitro*. Furthermore, if the compounds are available in a formulation that allows for delivery in animals, either orally or intravenously, the effects of the compounds could be tested *in vivo* in infected mice.

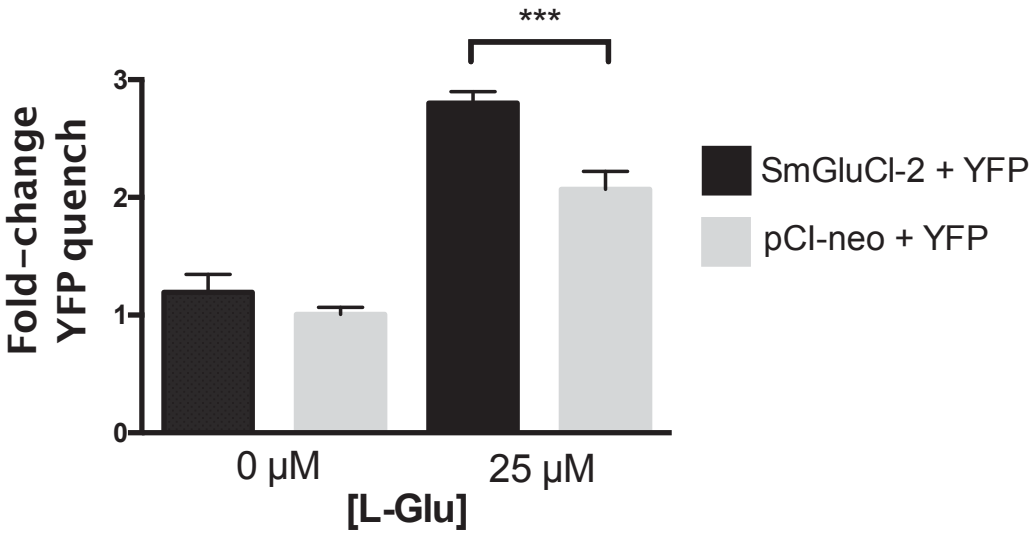

Figure 15. YFP fluorescence decrease in transfected HEK cells following L-glu application. HEK cells were transfected with either SmGluCl-2 and YFP or pCI-neo and YFP (mock transfected; control). Fluorescence levels were recorded pre- and post-L-glu application and the fold-change in YFP quench was determined. PBS acted as the no-drug control. $n \geq 4$; error bars represent SEM.

CONCLUSION

SmGluCl-4 may not form a functional glutamate receptor. However, the other subunits that do form receptors sensitive to L-glu should be explored as possible drug targets, especially considering the specificity of GluCls to invertebrates and the previous targeting of these types of channels in other parasites. Developing the mammalian cell assay will allow the properties of these channels to be explored further and could potentially lead to the discovery of a new anti-schistosomal compounds.

APPENDIX

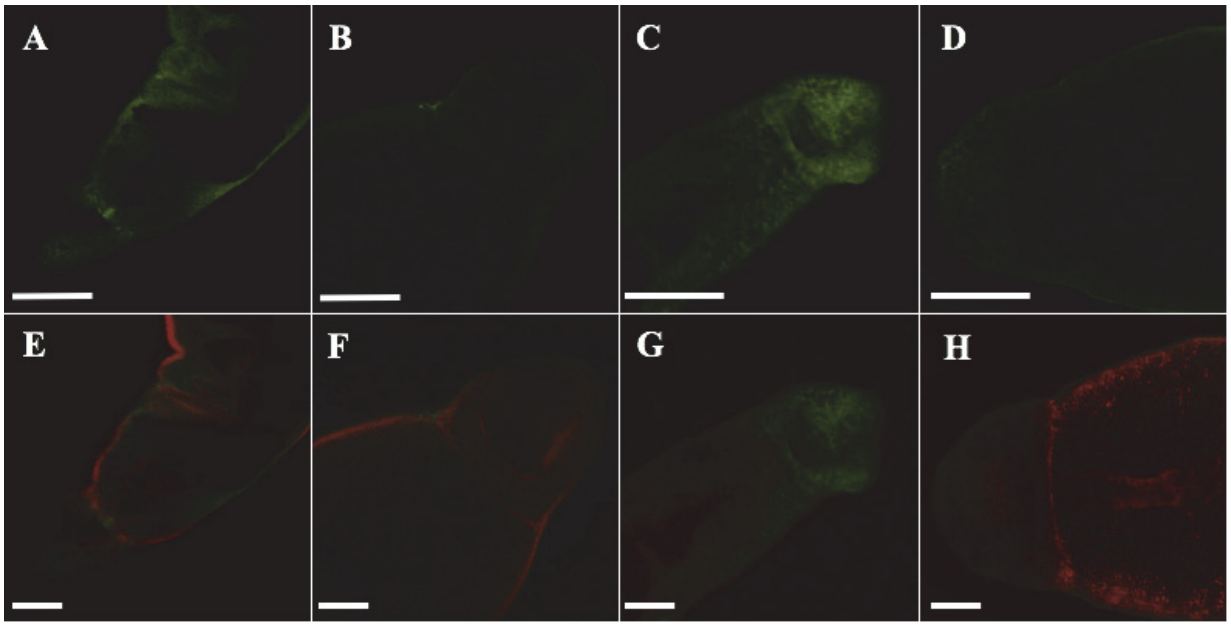

Figure A1. Negative controls for SmGluCl-4 localization. A, B. Female and male worms probed with secondary antibody only (AF-488 goat anti-rat; green) and counterstained with rhodamine-phalloidin (red). C, D. Female and male worms probed with primary antibody (rat anti-SmGluCl-4) pre-adsorbed with peptide antigen and secondary antibody and counterstained with rhodamine-phalloidin. E – H. Overlays corresponding images (above) with phalloidin counterstaining. Scale bar = 50 μM.

LITERATURE CITED

AGRAWAL, N., DASARDHI, P. V. N., MOHMMED, A., MALHOTRA., BHATNAGAR, R. K., MUKHERJEE, S. K. (2003). RNA interference: biology, mechanism, and applications. *Microbio Mol Bio Rev*. **67**, 657-685.

ANDREWS, A., THOMAS, H., POLKE, R. and SEUBERT, J. (1983). Praziquantel. *Med Res Rev*, **3**, 147-200.

ANGELUCCI, F., BASSO, M. BELLELLI, A., BRUNORI, M. PICA-MATTOCCIA, L. and VALE, C. (2007). The anti-schitosomal drug praziquantel is an adenosine antagonist. *Parasitol*, **134**, 1215-1221.

BARKER, L. R., BUEDING, E. and TIMMS, A. R. (1966). The possible role of acetylcholine in *Schistosoma mansoni*. *Br J Pharmac*, **26**, 656-665.

BECKER, B., MEHLHORM, H., ANDREWS, P., THOMAS, H. and ECKERT, L. (1980). Light and electron microscopic studies on the effect of praziquantel on *Schistosoma mansoni*, *Dicrocoelium dendriticum*, and *Fasciola hepatica* (Trematoda) in vitro. *Z Parasitenkd*, **63**, 113-128.

BERRIMAN, M., HAAS, B. J., LOVERDE, P. T., WILSON, R. A., DILLON, G. P., CERQUEIRA, G. C., MASHIYAMA, S. T., AL-LAZIKANI, B., ANDRADE, L. F., ASHTON, P. D., ASLETT, M. A., BARTHOLOMEU, D. C., BLANDIN, G., CAFFREY, C. R., CGHLAN, A., COULSON, R., DAY, T. A., DELCHER, A., DEMARCO, R., DJIKENG, A., EYRE, T., GAMBLE, J. A., GHEDIN, E., GU, Y., HERTZ-FOWLER, C., HIRAI, H., HIRAI, Y., HOUSTON, R., IVENS, A., JOHNSTON, D. A., LACERDA, D., MACEDO, C. D., MCVEIGH, P., NING, Z., OLIVEIRA, G., OVERINGTON, J. P., PARKHILL, J., PERTEA, M., PIERCE, R. J., PROTASIO, A. V., QUAIL, M. A., RAJADREAM, M. A., ROGERS, J., SAJID, D., SALZBERG, S. L., STANKE, M., TIVEY, A. R., WHITE, O., WILLIAMS, D .L., WORTMAN, J., WU, W., ZAMANIAN, M., ZERLOTINI, A., FRASER-LIGGETT, C. M., BARRELL, B. G. and EL-SAYED, N. M. (2009) The genome of the blood fluke *Schistosoma mansoni*. *Nature*, **460**, 352-358.

BOTROS, S. S. and BENNETT, J. L. (2007). Praziquantel resistance. *Expert Opin Drug Discov*, **2**, 35-40.

BOULIN, T., FAUVIN, A., CHARVET, C., CORTET, J., CABARET, J., BESSEREAU, J. L. AND NEVEU, C. (2011). Functional reconstitution of *Haemonchus contortus* acetylcholine receptors in *Xenopus* oocytes provides mechanistic insights into levamisole resistance. *Br J Pharmacol*, **164**, 1421-1432.

BOULIN, T., GIELEN, M., RICHMOND, J. E., WILLIAMS, D. C., PAOLETTI, P. AND BESSEREAU, J.-L. (2008). Eight genes are required for functional reconstitution of the *Caenorhabditis elegans* levamisole-sensitive acetylcholine receptor. *Proc Natl Acad*

Sci U.S.A., **105**, 18590–18595.

BROSNAN, J. T. AND BROSNAN, M. E. (2013). Glutamate: a truly functional amino acid. *Amino Acids*, **45**, 413-418.

BUEDING, E. (1952). Acetylcholinesterase activity of *Schistosoma mansoni*. *Br J Pharmac*, **7**, 563-566.

CAFFREY, C. R. (2007). Chemotherapy of schistosomiais: present and future. *Curr Opin Chem Biol*, **11**, 433-439.

CHANGEUX, J. P. (2010). Allosteric receptors: from electric organ to cognition. *Anny Rec Pharmacol Toxicol*, **50**, 1-38.

CHITSULO, L., ENGELS, D., MONTRESOR, A. and SAVIOLI, L. (2000). The global status of schistosomiasis and its control. *Acta Trop*, **77**, 41–51.

CIOLI, D., BOTROS, S. S., WHEATCROFT-FRANCKLOW, K., MBAYE, A., SOUTHGATE, V., TCHUEM TCHUENTE, L. A., PICA-MATTOCIA, L., TROIANI, A. R., SEIF EL-DIN, S. H., SABRA, A. N. A., ALBIN, J., ENGELS, D. and DOENHOFF, M. J. Determination of ED50 values for praziquantel in praziquantel-resistant and -susceptible *Schistosoma mansoni* isolates. *Int J Parasitol*, **34**, 979–987.

CIOLI, D. and PICA-MATTOCCIA, L. (2003). Praziquantel. *Parasitol Res,* **90,** 3–9.

COLLINS III, J. J. and NEWMARK, P. A. (2013). It's no fluke: The planarian as a model for understanding schistosomes. *PLos Pathog*, **9**, 1-5.

CUPP, E. W., SAUERBREY, M. and RICHARDS, F. (2011). Elimination of human onchocerciasis: history of progress and current feasibility using ivermectin (Mectizan((®))) monotherapy. *Acta Trop,* **120,** S100-S108.

DE VLAS, S. J. and GRYSEELS, B. (1992). Underestimation of *Schistosoma mansoni* prevalences. *Parasitol Today*, **8**, 274-277.

DENT, J. A. (2010). The evolution of pentameric ligand-gated ion channels. *Adv Exp Med Biol*, **683**, 11-23.

DOENHOFF, M. J., CIOLI, D. and UTZINGER, J. (2008). Praziquantel: mechanisms of action, resistance and new derivatives for schistosomiasis. *Curr Opin Infect Dis*, **21**, 659–667.

DOENHOFF, M. J. and PICA-MATTOCIA, L. (2006). Praziquantel for the treatment of schistosomiasis: its use for control in areas with endemic disease and prospects for drug resistance. *Expert Rev Anti Infect Ther*, **4**, 199-210.

DUFOUR, V. (2013). Molecular characterization of novel glutamate-gated chloride channel subunits from *Schistosoma mansoni* (Doctoral thesis, Institute of Parasitology, McGill University, Ste-Anne-de-Bellevue, Canada). Retrieved from http://digitool.Library. McGill.CA:80/R/-?func=dbin-jump-full&object_id=123127&silo_library=GEN01

DUFOUR, V., BEECH, R. N., WEVER, C., DENT, J. A. and GEARY, T. G. (2013). Molecular cloning and characterization of novel glutamate-gated chloride channel subunits from *Schistosoma mansoni. PLoS Pathog*, **9**, 1-14.

DUGUET, T. B., CHARVET, C. L., FORRESTERM S. G., WEVER, C. M., DENT, J. A., NEVEU, C. AND BEACH, R. N. (2016). Recent duplication and functional divergence in parasitic nematode levamisole-sensitive acetylcholine receptors. *PLoS Negl Trop Dis*, **10**, e0004826.

ENGELS, D., CHITSULO, L., MONTRESOR, A. and SAVIOLI, L. (2002). The global epidemiological situation of schistosomiasis and new approaches to control and research. *Acta Trop*, **82**, 139-146.

ENK, M. J., LIMA, A. C., DRUMMOND, S. C., SCHALL, V. T. and COELHO, P. M. (2008). The effect of the number of stool samples on the observed prevalence and infection intensity with *Schistosoma mansoni* among a population in an are of low transmission. *Acta Trop*, **108**, 222-228.

FALLON, P. G. (1998). Schistosome resistance to praziquantel. *Drug Resist Updat*, **1**, 236-241.

FALLON, P. G. and DOENHOFF, M. J. (1994). Drug-resistant schistosomiasis: resistance to praziquantel and oxamniquine induced in *Schistosoma mansoni* in mice is drug specific. *Am J Trop Med Hyg,* **51**, 83–88.

FALLON, P. G., STURROCK, R. F. CAPRON, A., NIANG, M. and DOENHOFF, M. J. (1995). Dimished susceptibility to praziquantel in a Senegal isolate of *Schistosoma mansoni. Am J Trop Med Hyg*, **53**, 61-62.

FENWICK, A. and WEBSTER, J. P. (2006). Schistosomiasis: challenges for control, treatment and drug resistance. *Curr Opin Infect Dis*, **19**, 577–582.

FENWICK, A., SAVIOLI, L., ENGELS, D., BERGQUIST, N. R., and TODD, M. H. (2003). Drugs for the control of parasitic diseases: current status and development in schistosomiais. *Trend Parasitol*, **19**, 509-515.

FITCH, R. W., XIAO, Y., KELLAR, K. J. AND DALY, J. W. (2003). Membrane potential fluorescence: a rapid and highly sensitive assay for nicotinic receptor channel function. *Proc Natl Acad Sci USA*, **100**, 4909-4914.

GALIETTA, L. J. V., HAGGIE, P. M. AND VERKMAN, A. S. (2001). Green fluorescent protein-based halide indicators with improved chloride and iodide affinities. *FEBS Lett*,

499, 220-224.

GALIETTA, L. J. V., JAYARAMANM, S. AND VERKMA, A. S. (2001). Cell-based assay for high throughput quantitative screening of CFTR chloride transport agonists. *Am J Physiol Cell Physiol*, **281**, 1734-1742.

GILBERT, D., ESMAEILI, A. AND LYNCH, J. W. (2009). Optimizing the expression of Recombinant αβγ $GABA_A$ receptors in HEK293 cells for high-throughput screening. *J Biomol Screen*, **14**, 86-91.

GREENBURG, R. M. (2005). Are Ca^{2+} channels targets of praziquantel action? *Int J Parasitol*, **35**, 1-9.

GREENBURG, R. M. (2014). Ion channels and drug transporters as targets for anthelmintics. *Curr Clin Micro Rpt*, **1**, 51-60.

GRYSEELS, B. (2012). Schistosomiasis. *Infect Dis Clin N Am*, **26**, 383–397.

GRYSEELS, B., POLMAN, K., CLERINX, J. and KESTENS, L. (2006). Human schistosomiasis. *Lancet*, **238**, 1106-1118.

HALTON, D. W. (1997) Nutritional adaptations to parasitism within the platyhelminths. *Int J Parasitol*, **27**, 693-704.

HALTON, D. W. and GUSTAFSSON, M. K. S. (1996). Functional morphology of the platyhelminth nervous system. *Parasitol*, **113**, S47-S72.

HALTON, D. W. and MAULE, A. G. (2004). Flatworm nerve-muscle: structural and functional analysis. *Can J Zool,* **82**, 316–333.

HAMS, E., AVIELLO, G. and FALLON, P. G. (2013). The *Schistosoma* granuloma: friend or foe? *Front Immunol*, **4**, 1-8.

HARRISON, R. R., KOLB, I., KODANDARAMAIAH, S. B., CHUBYKIN, A. A., YANG, A., BEAR, M. F., BOYDEN, E. S. AND FOREST, C. (2014). Microchip amplifier for *in vitro, in vivo*, and automated whole-cell patch-clamp recording. *J Neurophysiol*, **113**, 1275–1282.

HARNETT, W. and KUSEL, J. R. (1986). Increased exposure of parasite antigens at the surface of adult male *Schistosoma mansoni* exposed to praziquantel *in vitro*. *Parasitol,* **93**, 401–405.

HILLMAN, G. R. (1983). The neuropharmacology of schistosomes. *Pharmac, Ther,* **22**, 103-115.

HOPPE, P. S., COUTU, D. L. AND SCHROEDER, T. (2014). Single-cell technologies

sharpen up mammalian stem cell research. *Nat Cell Bio*, **16**, 919-927.

HOTEZ, P. J. and FERRIS, M. T. (2006) The antipoverty vaccine. *Vaccines*, **24**, 5787-5799.

ISMAIL, M., METWALLY, A., FARGHALY, A., BRUCE, J., TAO, L. F. and BENNETT, J. L. (1996). Characterization of isolates of Schistosoma mansoni from Egyptian villagers that tolerate high doses of praziquantel. *Am J Trop Med Hyg,* **55**, 214–218.

JOHANSSON, T., NORRIS, T. AND PEILOT-SJOGREN, H. (2013). Yellow fluorescent protein-based assay to measure $GABA_A$ channel activation and allosteric modulation in CHO-K1 cells. *PLoS ONE*, **8**, 1-7.

KING, C. H. and DANGERFIELD-CHA, M. (2008). The unacknowledged impact of chronic schistosomiasis. *Chronic Illn*, **4**, 65-79.

KRUGER, W., GILBERT, D., HAWTHORNE, R., HRYCIWA, D. H., FRINGS, S., PORRONIK, P. AND LYNCH, J. W. (2005). A yellow fluorescent protein-based assay for high-throughput screening of glycine and $GABA_A$ receptor chloride channels. *Neurosci Lett*, **380**, 340–345.

LOVERDE, P. T., NILES, E. G., OSMAN, A. and WU, W. (2004). *Schistosoma mansoni* male-female interactions. *Can J Zool*, **82**, 357-374.

LUI, J., CHEN, T., NORRIS, T., KNAPPENBERGER, K., HUSTON, J., WOOD, M. AND BOTSWICK, R. (2008). A high throughout functional assay for characterization of γ γ-aminobutyric $acid_A$ channel modulators using cryopreserved transiently transfected cells. *Assay Drug Devel Technol*, **6**, 781-786.

LYNAGH, T., BEECH, R. N., LALANDE, M. J., CROMER, B. A., WOLSTENHOLME, A. J. and LAUBE, B. (2015). Molecular basis for convergent evolution of glutamate recognition by pentameric ligand-gated ion channels. *Sci Rep*, **5**, 1-8.

LYNAGH, T. and LYNCH, J. W. (2010). A glycine residue essential for high ivermectin sensitivity in Cys-loop ion channel receptors. *Int J Parasitol*, **40**, 1477-1481.

LYNAGH, T. and LYNCH, J. W. (2012a). Ivermectin binding sited in human and invertebrate Cys-loop receptors. *Trends Pharmacol Sci*, **33**, 432-444.

LYNAGH, T. and LYNCH, J. W. (2012b). Molecular mechanisms of Cys-loop ion channel receptor modulation by ivermectin. *Front Mol Neurosci*, **5**, 1-11.

MACDONALD, K., BUXTON, S., KIMBER, M. J., DAY, T. A., ROBERTSON, A. P. AND RIBEIRO, P. (2014). Functional characterization of a novel family of acetylcholine-gated chloride channels in *Schistosoma mansoni*. *PLoS Pathog*, **10**, 1-14.

MEHLHORN, H., BECKER, B., ANDREWS, P., THOMAS, H. and FRENKEL, J. K. (1981).

In vivo and in vitro experiments on the effects of praziquantel on *Schistosoma mansoni*. *Drug Res*, **31**, 544-554.

MENDONÇA-SILVA, D. L., GARDINO, P. F., KUBRUSLY, R. C. C., DE MELLO, F. G. and NOËL, F. (2004). Characterization od GABAergic neurotransmission in adult *Schistosoma mansoni*. *Parasitol*, **129**, 137-146.

NASHMI, R., DICKINSON, M. E., MCKINNEY, S., JAREB, M., LABARCA, C., FRASER, S. E. AND LESTER, H. E. (2003). Assembly of α4ß2 nicotinic acetylcholine receptors assessed with functional fluorescently labeled subunits: effects of localization, trafficking, and nicotine-induced upregulation in clonal mammalian cells and in cultured midbrain neurons. *J Neurosci*, **23**, 11554-11567.

NATURAL HISTORY MUSEUM. (Accessed 2015). Biology of schistosomes and their host. http://www.nhm.ac.uk/research-curation/research/projects/schistosomes/

OLDS, G. R. and DASARATHY, S. (2000). Schistosomiasis. *Curr Treat Options Infect Dis*, **2**, 88-99.

OMASA, T., ONITSUKA, M. AND KIM, W.-K. (2010). Cell engineering and cultivation of Chinese hamster ovary (CHO) cells. *Curr Pharm Biotechnol*, **11**, 233-240.

PATOCKA, N., SHARMA, N., RASHID, M. and RIBEIRO, P. (2014). Serotonin signaling in *Schistosoma mansoni*: a serotonin-activated G protein-coupled receptor controls parasite movement. *PLoS Pathog*, **10**, 1-15.

PAX, R., BENNETT, J. L. and FETTERER, R. (1978). A benzodiazepine derivative and praziquantel effects on musculature of *Schistosoma mansoni* and *Schistosoma japonicum*. *Naunyn-Schiedberg's Arch Pharmacol*. **304**, 309-315.

PEARCE, E. J. and MACDONALD, A. S. (2002). The immunobiology of schistosomiasis. *Nat Rev Immunol*, **2**, 499-511.

POLONCHUK, L. (2012). Toward a new gold standard for early safety: automated temperature-controlled hERG test on the PatchLiner®. *Front Pharmacol*, **3**, 1-7.

PROTASIO, A. V., TSAI, I. J., BABBAGE, A., NICHOL, S., HUNT, M., ASLETT, M .A., DE SILVA, N., VELARDE, G. S., ANDERSON, T. J. C., CLARK, R. C., DAVIDSON, C., DILLON, G. P., HOLROYD, N. E., LOVERDE, P. T., LLOYD, C., MCQUILLAN, J., OLIVEIRA, G., OTTO, T. D., PARKER-MANUEL, S. P., QUAIL, M. A., WILSON, R. A., ZERLOTINI, A., DUNNE, D. W. and BERRIMAN, M. (2012). A systematically improved high quality genome and transcriptome of the human blood fluke *Schistosoma mansoni. PLoS Neglect Trop D*, **6**, 1-13.

RIBEIRO, P. and GEARY, T.G. (2010). Neuronal signaling in schistosomes: current status and prospects for postgenomics. *Can J Zool*, **88**, 1-22.

ROSENBERG, M. (2007). Global child health: Burden of disease, achievements, and future challenges. *Curr Probl Pediatr Adoles Health Care,* **37**, 338-262.

ROSS, A. G. P., BARTLEY, P. B., SLEIGH, A. C., OLDS, G. R., LI, Y., WILLIAMS, G. M. and MACMANUS, D. P. (2002). Schistosomiasis. *N Engl J Med*, **346**, 1212-1220.

SABRA, A. N. A. and BOTROS, S. S. (2008). Response of Schistosoma mansoni isolates having different drug sensitivity to praziquantel over several life cycle passages with and without therapeutic pressure. *J Parasitol,* **94**, 537–541.

SCELO, G. and BRENNAN, P. (2007) The epidemiology of bladder and kidney cancer. *Nat Clin Pract Urol*, **4**, 205-217.

SCI. (2008) Vol 2008 Department of infectios disease and epidemiology, Imperial College London, London.

SHAW, M. K. and ERASMUS, D. A. (1983). *Schistosoma mansoni:* Dose-related tegumental surface changes after *in vivo* treatment with praziquantel. *Parasitol Res*, **69**, 643-653.

SONNEWALD, U., WESTERGAARD, N. AND SCHOUSBOE, A. (1997). Glutamate transport and metabolism in astrocytes. *Glia*, **21**, 56-63.

STEINMANN, P., KEISER, J., BOS, R., TANNER, M. and UTZINGER, J. (2006). Schistosmiasis and water resources development: systematic review, meta-analysis, and estimates of people at risk. *Lancet Infect Dis*, **6**, 411–425.

STELMA, F. F., TALLA, I., SLOW, S., KONGS, A., NIANG, M., POLMAN, K., DEELDER, A.M. and GRYSEELS, B. (1995). Efficacy and side effects of praziquantel in an epidemic focus of *Schistosoma mansoni*. *Am J Trop Med Hyg,* **53**, 167–170.

STOKER, M. and MACPHERSON, I. (1964). Syrian hamster fibroblast cell line BHK21 and its derivatives. *Nature*, **203**, 1355-1357.

SUI, J., COTARD, S. ANDERSON, J., ZHU, P., STAUNTON, J., LEE, M. AND LIN, S. (2010). Optimization of a yellow fluorescent protein-based iodide influx high-throughput screening assay for cystic fibrosis transmembrane conductance regulator (CFTR) modulators. *Assay Drug Dev Technol*, **8**, 656-668.

TCHUEM TCHUENTE, L. A., SOUTHGATE, V. R., MBAYE, A., ENGELS, D. and GRYSEELS, B. (2001). The efficacy of praziquantel against *Schistosoma mansoni* infection in Ndombo, northern Senegal. *Trans R Soc Trop Med Hyg*, **95**, 65–66.

THOMSON, A. J., LESTER, H. A. and LUMMIS, S. C. (2010). The structural basis of function
in Cys-loop receptors. *Q Rev Biophy*, **43**, 449-499.

TOMOSKY, K. T., BENNETT, J. L. and BUEDING, E. (1974). Tryptaminergic and dopaminergic responses of *Schistosoma mansoni. J Pharmac Exp Ther,* **19**, 260-270.

UTZINGER, J., N'GORAN, E. K., CAFFREY, C. R. and KEISER, J. (2011). From innovation to application: social-ecological context, diagnostics, drugs and integrated control of schistosomiasis. *Acta Trop*, 120S, S121-S137.

VAN DEN ENDEN, E. (2009). Pharmacotherapy of helminth infection. *Expert Opin Pharmacother*, **10**, 435-451.

VERCRUYSSE, J. and REW, R. S. (2002). Macrocyclic lactones in antiparasitic therapy. *CABI Publishing.*

WANG, X. AND MIN, L. (2003). Automated electrophysiology: high-throughput of art. *Assay Drug Dev Technol*, **1**, 695-708.

WHO. (2001). Report of the informal consultation on schistosomiasis in low transmission areas: control strategies and criteria for elimination.

WHO. (2011). Schistosomiasis progress report 2001-2011 and strategic plan 2012-2020.

WOLSTENHOLME, A. J. (2012) Glutamate-gated chloride channels. *J Biol Chem*, **287**, 40232-40238.

YE, Z. C. and SONTHEIMER, H. (1998). Astrocytes protect neurons from neurotoxic injury by serum glutamate. *Glia*, **22**, 237-248.

ZEMKOVA, H., TVRDONOCA, V., BHATTACHARYA, A. and JINDRICHOVA, M. (2014). Allosteric modulation of ligand gated ion channels by ivermectin. *Physiol Res*, **63**, 215-224.